Gravitational radiation reaction for bound motion around a Schwarzschild black hole

Curt Cutler*
Center for Radiophysics and Space Research, Cornell University, Ithaca, New York 14853

Daniel Kennefick and Eric Poisson†
Theoretical Astrophysics, California Institute of Technology, Pasadena, California 91125
(Received 11 May 1994)

A particle of mass μ moves, in the absence of external forces, in the geometry of a nonrotating black hole of mass M. The system (black hole plus particle) emits gravitational waves, and the particle's orbit evolves under radiation reaction. The aim of this paper is to calculate this evolution. Our calculations are carried out under the assumptions that $\mu/M \ll 1$, that the orbit is bound, and that radiation reaction takes place over a time scale much longer than the orbital period. The bound orbits of the Schwarzschild spacetime can be fully characterized, apart from initial conditions, by two orbital parameters: the semi-latus rectum p, and the eccentricity e. These parameters are so defined that the turning points of the radial motion (the values of the Schwarzschild radial coordinate at which the radial component of the four-velocity vanishes) are given by $r_1 = pM/(1+e)$ and $r_2 = pM/(1-e)$. The units are such that $G = c = 1$. We use the Teukolsky perturbation formalism to calculate the rates at which the gravitational waves generated by the orbiting particle remove energy and angular momentum from the system. These are then related to the rates of change of p and e, which determine the orbital evolution. We find that the radiation reaction continually decreases p, in such a way that the particle eventually plunges inside the black hole. Plunging occurs when p becomes smaller than $6+2e$. (Orbits for which $p < 6+2e$ do not have a turning point at $r = r_1$.) For weak-field, slow-motion orbits (which are characterized by large values of p), the radiation reaction decreases e also. However, for strong-field, fast-motion orbits (small values of p), the radiation reaction *increases* the eccentricity if p is sufficiently close to its minimum value $6+2e$. The change of sign of de/dt can be interpreted as a precursor effect to the eventual plunging of the orbit.

PACS number(s): 04.30.Db, 04.25.Dm, 97.60.Lf

I. INTRODUCTION AND SUMMARY

A. The problem

A particle of mass μ moves, in the absence of external forces, in the gravitational field of a nonrotating black hole of mass M. It is assumed that the motion is bound, and that $\mu \ll M$, but no restriction is put on the strength of the gravitational field at the particle's location: the field is arbitrarily strong, and the motion arbitrarily fast. The system (black hole plus particle) possesses a time-varying mass distribution, and therefore emits gravitational waves. These waves remove energy and angular momentum from the system. The question we intend to tackle in this paper is the following: How does the system react to the emission of gravitational waves? Or more precisely: What is the orbital evolution under the influence of gravitational radiation reaction?

The present work complements and generalizes two previous analyses: one by Apostolatos, Kennefick, Ori, and Poisson [1], the other by Tanaka, Shibata, Sasaki, Tagoshi, and Nakamura [2].

Apostolatos *et al.* [1] considered the evolution, under gravitational radiation reaction, of slightly eccentric orbits in the Schwarzschild spacetime. This paper generalizes that work by considering the evolution of *any* bound orbit. In the language to be introduced in Sec. ID, the results of Apostolatos *et al.* can be recovered by taking the $e \to 0$ limit of those presented here.

Tanaka *et al.* [2] have also considered a wide class of bound orbits, and have therefore contributed significantly to the problem treated here. This paper extends and complements their work by providing (i) a useful language in which to describe the results (the p-e plane, to be introduced in Sec. ID); (ii) analytical results which apply, approximately, to some interesting regions of the p-e plane; and (iii) a discussion which is focused entirely on the radiation reaction, rather than on the fluxes of energy and angular momentum at infinity, which is the main focus of Tanaka *et al.*

B. Motivation

The chief motivation for this work comes from the desire to achieve a deeper understanding of gravitational

*Present address: Center for Gravitational Physics and Geometry, Pennsylvania State University, University Park, PA 16802.
†Present address: Department of Physics, Washington University, St. Louis, MO 63130.

radiation reaction in the relativistic two-body problem, especially in situations where the gravitational field is strong, and the motion fast. (For an overview of the two-body problem in general relativity, see Ref. [3] and references therein.)

For weak fields and slow motions, the physics of gravitational radiation reaction is well understood [3–9]. In this context, calculations are carried out using post-Newtonian theory [10], and the equations of motion are derived accurately to some order in v/c. Here, v is the orbital velocity and c the speed of light. To leading order in post-Newtonian theory [11], the radiation reaction is taken into account by adding a piece $\Phi_{\rm rr}$ to the Newtonian potential [4,5]. Post-Newtonian corrections to the radiation-reaction force have recently been calculated by Blanchet [8] and by Iyer and Will [9].

Because the post-Newtonian expansion is presumably only asymptotic, and not convergent [3,10], it is not clear that post-Newtonian theory will ever succeed in providing an accurate description of the radiation reaction in situations where v/c is not small. To understand the strong-field effects, it is therefore useful to employ an alternative approach. Although limited to the case of orbital motion around a nonrotating black hole, this paper presents concrete results on radiation reaction in strong fields.

Because of the restriction $\mu \ll M$, the results presented in this paper are not directly applicable to the inspiral, and final coalescence, of a compact binary system of two comparable masses [12]. This problem will have to be solved using either post-Newtonian theory, or the techniques of numerical relativity which are currently under intense development [13]. However, it is conceivable that certain features of the small-mass-ratio orbital evolution will also be present in the more general case. (One such feature, the increase of the orbital eccentricity during the last stages of the inspiral, will be discussed below.) We may therefore hope that the results presented here will eventually be useful for interpretation purposes, when the evolution of binary systems with large mass ratios is better understood. In the meantime, our results will provide useful ways to check other methods of analysis, including post-Newtonian theory and numerical relativity.

Additional motivation for our work comes from the possibility that gravitational waves generated by the capture of solar-mass compact stars by supermassive black holes residing in galactic nuclei may be observed by eventual space-borne detectors, such as the proposed LISA (Laser Interferometer Space Antenna) project [14]. Such detectors are designed to operate in the frequency band between 10^{-3} Hz and 10^{-1} Hz, so that the waves emitted during the last stages of the capture are observable only if the central black hole has a mass ranging from $10^4 M_\odot$ to $10^6 M_\odot$. To avoid tidal disruption by the black hole [15], the captured star must be compact (a white dwarf, a neutron star, or a black hole).

Stars, normal or compact, are continually injected, by N-body processes, toward the vicinity of the central black hole, where they lose orbital energy and angular momentum to gravitational waves [16]. Eventually the star interacts solely with the black hole, and the orbital evolution becomes dominated by gravitational radiation reaction. Because these systems have small mass ratios, and because it can be expected that the stars move on highly eccentric orbits following their capture [16], the results presented in this paper are directly relevant to these sources of gravitational waves.

The application of our work to the capture of solar-mass compact objects by supermassive black holes will be the subject of a separate publication [17].

C. Method of solution

There currently exists no prescription to calculate the radiation reaction force acting on a (pointlike or extended) particle moving in a given background gravitational field, excluding the well-understood case of weak fields and slow motions. (We will return to this point, and discuss Gal'tsov's proposal for such a prescription [18], in Sec. I F.) Nevertheless, the problem considered in this paper can be tackled using a rather simple-minded approach, which we now describe.

A particle of mass μ moves, in the absence of external forces, in the geometry of a nonrotating black hole, and slightly perturbs the hole's gravitational field. The total field can be calculated by solving Einstein's equations perturbatively about the Schwarzschild solution [19]. The resulting equations take the form of linear wave equations for the perturbations, with the particle's stress-energy tensor acting as a source. The perturbations propagate away from the source as gravitational waves, and carry with them energy and angular momentum. Solving the perturbation equations allows us to calculate the rates at which energy and angular momentum are removed from the system (black hole plus particle).

The timelike geodesics of the Schwarzschild spacetime (Sec. II A) can be fully characterized, apart from initial conditions, by two orbital parameters, $\tilde{E}$ the orbital energy per unit mass, and $\tilde{L}$ the orbital angular momentum per unit mass. (Here, the mass is that of the particle.) The rates at which these quantities change with time are obtained from the solutions to the perturbation equations, and the orbital evolution under radiation reaction is determined.

Such a calculation can easily be carried out if the two following conditions hold. First, the gravitational perturbations produced by the orbiting particle must have small amplitudes. This is to ensure that the nonlinearities of the perturbation fields can, to sufficient accuracy, be ignored. This will be the case if the inequality $\mu/M \ll 1$ is enforced.

Second, we must require that the orbits change very little over time scales which are comparable to the orbital period. This is because the source term in the wave equations—the stress-energy tensor, which depends on the particle's world line—must be specified before the equations are integrated. The motion of the particle must therefore be specified during the time interval over which the wave equations are integrated. And because the or-

bital motion is essentially periodic (Sec. II D), this time interval can be set equal to the orbital period. This procedure is self-consistent only if radiation reaction occurs over a time scale much longer than the orbital period, which shall be assumed here. This *adiabatic approximation* can be imposed by formulating additional constraints on the size of μ/M. These constraints will be derived in Sec. IV D.

When the adiabatic approximation is valid, the calculation proceeds as follows. We begin by assuming that the motion is strictly geodesic over several orbital periods, and we evaluate the particle's stress-energy tensor. We then compute, by integrating the wave equations, $\langle d\tilde{E}/dt\rangle$ and $\langle d\tilde{L}/dt\rangle$, the *time-averaged* rates of change of the orbital parameters. (The average is taken over several orbital periods.) Finally, we infer from these quantities the slow, secular evolution of the orbit. Provided that μ/M is suitably constrained, the results are compatible with the initial assumption, and the calculation is self-consistent.

In this paper the gravitational perturbations are described using the Teukolsky formalism [20], in which all information about the perturbations is contained in the complex-valued function Ψ_4, a particular component of the Weyl tensor. In this formalism, a single wave equation needs to be solved, and the rates at which energy and angular momentum are carried away can easily be obtained from the solution. The Teukolsky formalism will be reviewed briefly in Sec. III B.

D. Orbital parameters

The evolution, under radiation reaction, of the bound orbits of the Schwarzschild spacetime can best be described in terms of a set of orbital parameters which is different from the set $\{\tilde{E}, \tilde{L}\}$. For this purpose we introduce p, the orbit's semi-latus rectum, and e, its eccentricity. Both p and e are dimensionless, and are regular functions of $\tilde{E}$ and $\tilde{L}$. (See Sec. II B below, which contains a more detailed presentation.)

The new orbital parameters are defined as follows. For bound orbits, the radial motion (the evolution of the Schwarzschild radial coordinate r as a function of proper time τ) takes place between two turning points (the values of r at which $dr/d\tau = 0$). We denote the periastron by r_1 and the apastron by r_2, so that $r_1 \leq r_2$. We define p and e such that $r_1/M = p/(1+e)$ and $r_2/M = p/(1-e)$, using units in which $G = c = 1$. The semi-latus rectum therefore measures the size of the orbit, while the eccentricity measures its degree of noncircularity.

The bound orbits of the Schwarzschild spacetime can be represented by those points in the p-e plane (Fig. 1) which satisfy the inequalities $0 \leq e < 1$, $p \geq 6 + 2e$. Points for which $p < 6 + 2e$ represent plunging orbits (these do not have a turning point at $r = r_1$). The boundary $p = 6+2e$ will be referred to as the *separatrix*. Points on the p axis represent *stable* circular orbits, which have vanishing eccentricity. Points on the separatrix represent *unstable* circular orbits, for which $e \neq 0$.

In the absence of radiation reaction, p and e are constants of the motion. In the presence of radiation reaction, p and e evolve slowly, over a time scale long compared with the orbital period. The evolution of a given orbit therefore traces a trajectory in the p-e plane. (The p-e plane can be regarded as a phase space, and the trajectories as phase curves.) Our goal in this paper is to calculate the radiation-reaction trajectories.

E. The results

It is most convenient to represent the radiation-reaction trajectories, or phase curves, in terms of a phase diagram, in which the tangent vectors $(\dot{p}, \dot{e})$—the phase velocity field—are plotted. (Here and throughout, a dot denotes differentiation with respect to time followed by an average over several orbital periods.) Such a representation is given in Fig. 1. The results can also be expressed in terms of the function $c(p, e)$, where

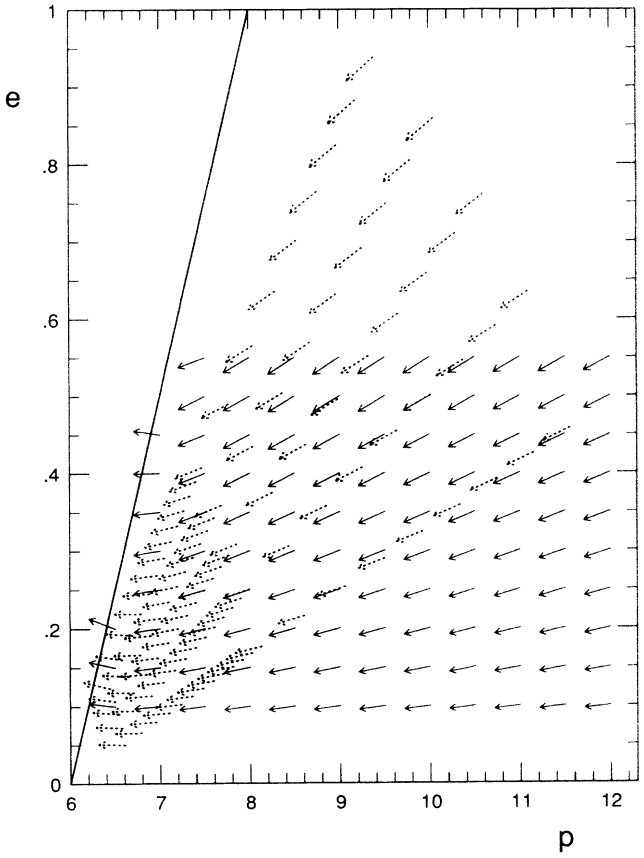

FIG. 1. The bound orbits of the Schwarzschild spacetime can be represented by points in the p-e plane, a portion of which is depicted here. The solid, diagonal line to the left is the separatrix $p = 6 + 2e$. The bound orbits are located to the right of the separatrix. Radiation reaction produces a slow evolution of the orbital parameters, and therefore generates curves in the p-e plane. These can be parametrized by p and have $\mathbf{v} = (1, de/dp)$ as tangent vectors. The vector field $\mathbf{v}(p, e)$ is also plotted here, with each point (p, e) located at the arrow's tail end. For convenience we have uniformly rescaled the length of the vectors. The solid arrows represent the calculations of this paper. The dotted arrows represent the results of Tanaka *et al.* [2].

$$c(p,e) = \frac{d\ln e}{d\ln p}. \tag{1.1}$$

In Fig. 2 we have provided a three-dimensional plot of $c(p,e)$ for the most interesting range of orbital parameters.

Before we proceed with a summary of our main results we must first recall one of the main conclusions of Ref. [1]: If an orbit has a vanishing eccentricity initially, then the radiation reaction does not change the value of the eccentricity. In other words, circular orbits remain circular under radiation reaction. [This statement follows directly from Eq. (4.15) below, which implies that $\dot{e} \propto e$ for small eccentricities.] In such circumstances, the value of p slowly decreases until $p = 6$ is reached, at which point the particle plunges inside the black hole.

We now discuss the more general case of orbits possessing nonvanishing eccentricities, first describing the results which were obtained using analytical methods.

We begin with a discussion of weak-field situations (Sec. IV A), that is, orbits with large values of p. In this case we find that $\dot{p} < 0$, $\dot{e} < 0$, and

$$c(p \to \infty, e) \sim \tfrac{19}{12}\left(1 + \tfrac{7}{8}e^2\right)^{-1}\left(1 + \tfrac{121}{304}e^2\right), \tag{1.2}$$

which is valid up to fractional corrections of order p^{-1}. These conclusions recover the well-known result that weak-field radiation reaction decreases both the size of the orbit and its eccentricity [21,22]. In Ref. [1], the first post-Newtonian corrections to Eq. (1.2) were calculated for the case of small eccentricities. For completeness we quote this result here:

$$c(p \to \infty, e \ll 1) = \tfrac{19}{12}\Big[1 - \tfrac{3215}{3192}p^{-1} + \tfrac{377}{152}\pi p^{-3/2} + O(p^{-2}, e^2)\Big]. \tag{1.3}$$

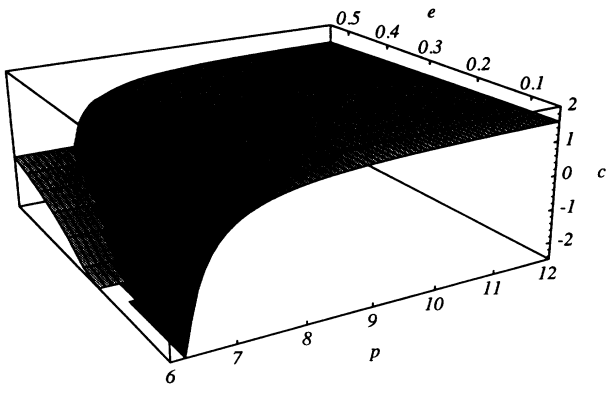

FIG. 2. A three-dimensional plot of the function $c(p,e) = d\ln e/d\ln p$, for the range $6 \le p \le 12$ and $0 \le e \le 0.55$. The function $c(p,e)$ is not defined for $p < 6+2e$. In this region we have plotted $\hat{c}(p,e) = -(1-e)/e$, which is equal to $c(p,e)$ at $p = 6 + 2e$; see Eq. (1.4). The intersection of the surface $c = c(p,e)$ with the plane $c = 0$ defines the critical curve, along which $de/dp = 0$; see Fig. 3. The value of $c(p,e)$ at the point $(7.5, 0.5)$ appears anomalous, but there is no reason to suspect the accuracy of our results at that point.

We next turn to cases for which the gravitational field is extremely strong. More precisely, we now consider points in the p-e plane which are very close to the separatrix $p = 6+2e$. (In this region, the validity of the adiabatic approximation implies severe restrictions on μ/M; see Sec. IV D.) It is also possible, for such orbits, to calculate the radiation reaction analytically (Sec. IV B). We find that when the inequality $p - 6 - 2e \ll \min(1, 4e)$ is satisfied [a more precise version of this condition is given by Eqs. (2.23) and (2.30) below], then $\dot{p} < 0$, $\dot{e} > 0$, and

$$c(p \to 6 + 2e, e \gg \varepsilon/4) \sim -\frac{1-e}{e}. \tag{1.4}$$

Here, $\varepsilon \equiv p - 6 - 2e$, and Eq. (1.4) is valid up to fractional corrections of order $(\varepsilon/4e)\ln(\varepsilon/4e)$.

Equation (1.4) is valid for small eccentricities *provided* that $\varepsilon \ll 4e$. This amounts to approaching the point $(p,e) = (6,0)$ along a path which lies very close to the separatrix. The result is different if we approach the point $(6,0)$ in a different direction. For example, if we choose a path which lies very close to the p axis (Sec. IV C), so that $e \ll p - 6$, then we find that $\dot{p} < 0$, $\dot{e} > 0$, and

$$c(p \to 6, e \ll p - 6) \sim -\tfrac{3}{2}(p-6)^{-1}, \tag{1.5}$$

which is valid up to fractional corrections of order $\max[p-6, e^2/(p-6)^2]$. Equation (1.5) was first derived in Ref. [1]. Equations (1.4) and (1.5) imply that the point $(6,0)$ is, in some sense, a singularity of the p-e plane. Not only does $c(p,e)$ diverge at that point, but its degree of divergence depends on the direction of approach.

We remark at the end of Sec. IV C that Eqs. (1.4) and (1.5), but not Eqs. (1.2) and (1.3), are in fact valid for *any* type of radiation field.

Equations (1.4) and (1.5) both imply that near the separatrix, the radiation reaction *increases* the eccentricity: $\dot{e} > 0$ everywhere near $p = 6 + 2e$ [23]. This is in marked contrast with weak-field situations, for which the eccentricity always decreases. This result, that gravitational radiation reaction increases the eccentricity if p is sufficiently close to $6 + 2e$, is the main conclusion of this paper. (This discovery was first made by Tanaka *et al.* [2]. Our contribution is the analytical proof that this occurs for *any* eccentricity.)

The asymptotic expressions for $c(p,e)$, Eqs. (1.2)–(1.5), taken together, imply the existence of a *critical curve* in the p-e plane, along which $de/dp = 0$. Equation (1.4) further implies that the critical curve meets with the separatrix at $e = 1$. A portion of the critical curve is displayed in Fig. 3.

The evolution of an orbit under gravitational radiation reaction typically proceeds as follows (Fig. 1). Suppose that the orbit lies initially in the weak-field region, so that $p \gg 6$. Radiation reaction slowly decreases both p and e, until the orbit crosses the critical curve and the eccentricity reaches its minimum. From then on, the radiation reaction continues to decrease p, but now increases e. Finally, the orbit reaches the separatrix, and the particle plunges inside the black hole.

Because the critical curve lies relatively close to the separatrix, the change of sign of $\dot{e}$—a genuine strong-field effect—can be interpreted as a precursor effect to the eventual plunging of the orbit.

The results represented in Figs. 1–3 were obtained numerically. We will describe our numerical methods in Sec. V below.

F. Future work

The techniques used in this paper could readily be extended to the case of a particle moving in the equatorial plane of a Kerr black hole. This is because the equatorial orbits of the Kerr spacetime can also be fully characterized by two orbital parameters. The radiation reaction can therefore be calculated in the same way.

The same cannot be said of orbits in Kerr which lie outside the equatorial plane. These orbits are characterized by three orbital parameters: orbital energy, orbital angular momentum, and the Carter constant [24]. There is no known relation—and it is not even clear whether one exists—between the rate of change of the Carter constant and the fluxes of energy and (vectorial) angular momentum carried by the gravitational waves. It is therefore unlikely that this most general problem will be solved before the elaboration of a robust formalism for strong-field, fast-motion radiation reaction [25].

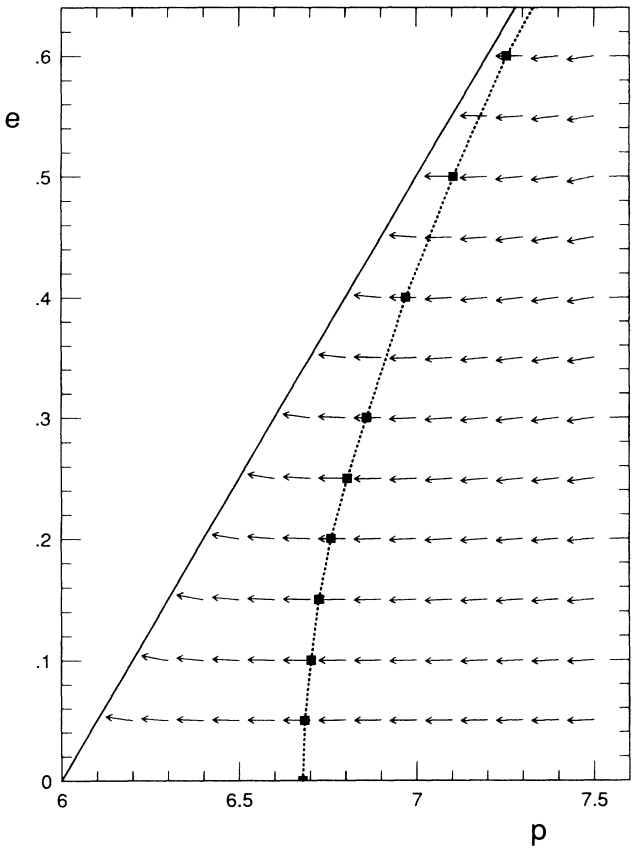

FIG. 3. A portion of the p-e plane in which lies a portion of the critical curve (along which $de/dp = 0$). The solid, diagonal line to the left is the separatrix. The solid squares represent points on the critical curve. (The thickness of the squares exceeds the numerical uncertainty.) The dotted curve consists of straight line segments joining these points. The arrows have the same meaning as in Fig. 1. Arrows to the right of the critical curve point down, indicating that radiation reaction decreases the eccentricity. Arrows to the left of the critical curve point up, indicating that radiation reaction increases the eccentricity.

Conceivably, such a formalism could be constructed along the lines of DeWitt and Brehme's derivation [26] of the curved spacetime version of the Lorentz-Dirac equation [27]. The problem to be solved is a generalization of the one examined in this paper. A particle of mass μ moves in the (arbitrary but known) gravitational field $g_{\alpha\beta}$ of an isolated mass M. (The prototype metric is the Kerr solution, but the problem may be formulated more generally.) To first order in μ/M, which is assumed small, what are the equations that the motion of the particle satisfies? (To zeroth order, the particle follows a geodesic of $g_{\alpha\beta}$; to first order, the system emits gravitational waves and radiation reaction takes place.)

This problem appears tractable, because the small perturbations produced by the particle obey linear wave equations in the background field $g_{\alpha\beta}$, and these wave equations can be formally integrated with the help of retarded Green's functions [26]. Because the Green's functions have support both on and inside the light cone, the resulting radiation-reaction force will depend both on the instantaneous state of the particle, and on its entire past history.

Gal'tsov has already proposed [18], for the special case of the Kerr metric, a radiation-reaction formalism based on solutions to the Teukolsky equation [20] of the half retarded minus half advanced type. But because of the causal structure of the Green's functions, the radiation-reaction force constructed in this way depends not only on the particle's past history, but also on its future history. (This is because the advanced Green's function has support inside the future light cone of the field point.) It is therefore not clear whether the Gal'tsov formalism is suitable for calculating the evolution of the nonequatorial orbits [28]. However, it should be quite adequate for the special case of *periodic* orbits [28], for which the past and future histories are identical (apart from the slow evolution due to radiation reaction).

G. Organization of the paper

The rest of the paper is devoted to the derivation of the results summarized in Sec. I E.

We begin in Sec. II with a detailed study of the bound orbits of the Schwarzschild spacetime. Most of the material presented in this section is not new, but for convenience the discussion is essentially self-contained. The geodesic equations are written, and the orbital parameters $\tilde{E}$ and $\tilde{L}$ defined, in Sec. II A. In Sec. II B we introduce the semi-latus rectum p and the eccentricity e, and we describe the bound orbits of the Schwarzschild space-

time in terms of the p-e plane. In Sec II C we provide a method for integrating the geodesic equations which is well suited both for analytic and numerical calculations. The two fundamental frequencies of the motion, the radial frequency Ω_r, and the azimuthal frequency Ω_ϕ, are defined in Sec. II D. In Sec. II E we integrate the geodesic equations for the special case $\varepsilon \equiv p - 6 - 2e \ll \min(1, 4e)$, and derive analytical expressions for Ω_r and Ω_ϕ. In Sec. II F we do the same for the special case $e \ll \min(1, p-6)$.

In Sec. III we describe our radiation-reaction formalism in detail. We explain the basic method in Sec. III A, and review the Teukolsky perturbation formalism [20] in Sec. III B. In particular, we show how to infer $\dot{E}$ and $\dot{L}$, the rates at which the gravitational waves carry energy and angular momentum to infinity, from the solution to the Teukolsky equation. (We will ignore, in this paper, the energy and angular momentum which are absorbed by the black hole. This will be justified in Sec. V E. However, these contributions *are* included in our analytical calculations.) In Sec. III C we calculate the source to the Teukolsky equation, and we formally integrate that equation in Sec. III D. In Sec. III E we derive equations relating the rates of change of p and e to $\dot{E}$ and $\dot{L}$, and explain why the radiation-reaction trajectories (the phase curves of Sec. I D) must cross the separatrix $p = 6 + 2e$.

Section IV is devoted to the derivation of our analytical results, in particular, Eqs. (1.2), (1.4), and (1.5). Weak-field situations are considered in Sec. IV A, while the strong-field results are derived in Sec. IV B [for the case $\varepsilon \ll \min(1, 4e)$] and C (for the case $4e \ll \varepsilon \ll 1$). In Sec. IV D we formulate constraints on μ/M which ensure the validity of the adiabatic approximation.

Finally, in Sec. V, we describe the numerical methods which were used to obtain the results presented in Figs. 1–3. We begin with a brief description of the numerical task in Sec. V A, and then discuss various aspects of it in Secs. V B–D. In Sec. V E we estimate the overall accuracy of our results, and compare them to those of Tanaka *et al.* [2].

II. BOUND ORBITS OF THE SCHWARZSCHILD SPACETIME

This section is devoted to the study of the bound orbits of the Schwarzschild spacetime. Most of the material presented here is not new, and can be found in the classic papers of Hagihara [29] and Darwin [30], or in Chandrasekhar's book [19]. The main purpose of this section is to establish the notation used in the rest of the paper; it will also serve as a repository of various useful results. For convenience, the material is presented in an entirely self-contained manner.

A. The geodesic equations

The timelike geodesics of the Schwarzschild spacetime are described by the equations

$$\begin{aligned} dt/d\tau &= \tilde{E}/f, \\ d\phi/d\tau &= \tilde{L}/r^2, \\ (dr/d\tau)^2 &+ V(\tilde{L}, r) = \tilde{E}^2; \end{aligned} \tag{2.1}$$

we have put $\theta = \pi/2$ without loss of generality. Here, the coordinates $\{t, r, \theta, \phi\}$ are the usual Schwarzschild coordinates, and τ is the particle's proper time; $\tilde{E}$ and $\tilde{L}$ are constants of the motion, respectively, the orbital energy and angular momentum, both divided by μ, the mass of the particle. We have also defined $f = 1 - 2M/r$, where M is the mass of the black hole (it is assumed that $\mu \ll M$), and the effective potential for radial motion is given by

$$V(\tilde{L}, r) = f(1 + \tilde{L}^2/r^2). \tag{2.2}$$

The qualitative behavior of the effective potential is represented in Fig. 4.

B. Orbital parameters: p and e

Apart from initial conditions, the orbits of the Schwarzschild spacetime are completely characterized by the values of two orbital parameters, which can be chosen to be $\tilde{E}$ and $\tilde{L}$. Bound motion occurs if

$$\tilde{E} < 1, \qquad \tilde{L} \geq 2\sqrt{3}M. \tag{2.3}$$

When $\tilde{E}$ and $\tilde{L}$ satisfy Eq. (2.3), the equation $V(\tilde{L}, r) = \tilde{E}^2$ possesses in general three distinct roots, which we designate by $r_3 \leq r_1 \leq r_2$. This situation is depicted in Fig. 4. The motion takes place between the turning points r_1 (the periastron) and r_2 (the apastron). We are not concerned with the plunging motion occurring inside $r = r_3$.

We define p, the *semi-latus rectum* and e, the *eccentricity*, such that

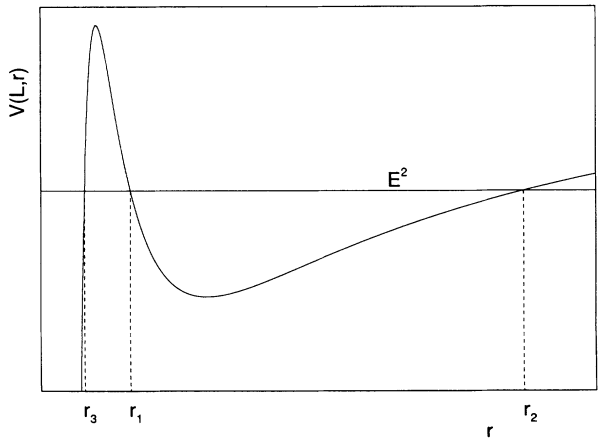

FIG. 4. The effective potential for radial motion. The three turning points $r_3 \leq r_2 \leq r_1$ are defined by the cubic $V(\tilde{L}, r) = \tilde{E}^2$. Bound motion takes place between r_1, the periastron, and r_2, the apastron.

$$r_1 = \frac{pM}{1+e}, \quad r_2 = \frac{pM}{1-e}. \tag{2.4}$$

Both p and e are dimensionless. As implied by Eq. (2.4), p measures the size of the orbit, while e measures its degree of noncircularity. These quantities have been used previously by Darwin [30]. Notice that e is confined to the range $0 \leq e < 1$; the value of p will be constrained below.

The relationship between $\{p, e\}$ and $\{\tilde{L}, \tilde{E}\}$ can be obtained by comparing the cubic $V(\tilde{L}, r) = \tilde{E}^2$ to its equivalent form $(r - r_1)(r - r_2)(r - r_3) = 0$. This yields $r_3/M = 2p/(p-4)$,

$$\tilde{E}^2 = \frac{(p-2-2e)(p-2+2e)}{p(p-3-e^2)}, \tag{2.5}$$

and

$$\tilde{L}^2 = \frac{p^2 M^2}{p-3-e^2}. \tag{2.6}$$

The inequalities (2.3) are then automatically satisfied for any value of p, and for any $e < 1$.

Stable circular orbits occur when $\tilde{E}^2$ is equal to the minimum value of the effective potential. This implies $r_1 = r_2$, so that

$$\text{stable circular orbits} \quad \Leftrightarrow \quad e = 0. \tag{2.7}$$

The radius of a stable circular orbit is equal to pM.

Unstable circular orbits occur when $\tilde{E}^2$ is equal to the maximum value of the effective potential. The turning points r_1 and r_3 are then no longer distinct, and the condition $r_1 = r_3$ does *not* correspond to zero eccentricity. Instead,

$$\text{unstable circular orbits} \quad \Leftrightarrow \quad p = 6 + 2e. \tag{2.8}$$

The radius of an unstable circular orbit is equal to $(6 + 2e)M/(1+e)$.

It is easy to see that p must satisfy the inequality $p \geq 6 + 2e$ in order for the orbit to be bound; otherwise the orbit is a plunging one, with a unique turning point at $r = r_2$. It is worth noting that this inequality implies $r_1/M \geq (6+2e)/(1+e)$; the periastron radius is therefore always larger than $4M$. We also remark that the curves $p = 6 + 2e$ and $e = 0$ meet at $p = 6$, which implies that stable circular orbits occur only for $p > 6$.

The bound orbits of the Schwarzschild spacetime can be represented by those points in the p-e plane which satisfy the inequalities $0 \leq e < 1$, $p \geq 6 + 2e$. The boundary $p = 6 + 2e$ will be referred to as the *separatrix*.

C. Integration of the geodesic equations

We integrate Eqs. (2.1) by eliminating τ from the system of equations, and by choosing r as the parameter along the orbit. Clearly r is a multivalued parameter, and the radial motion possesses two distinct branches. We take the first branch to be the motion from r_1 to r_2, and the second branch to be the motion from r_2 back to r_1.

Integrating Eqs. (2.1) gives

$$t(r) = \begin{cases} \hat{t}(r) & \text{first branch,} \\ P - \hat{t}(r) & \text{second branch,} \end{cases} \tag{2.9}$$

where

$$\hat{t}(r) = \tilde{E} \int_{r_1}^{r} \frac{dr'}{f'(\tilde{E}^2 - V')^{1/2}}, \tag{2.10}$$

with $f' = 1 - 2M/r'$ and $V' = V(\tilde{L}, r')$. We have also defined $P = 2\hat{t}(r_2)$, the period of the radial motion. Similarly we find

$$\phi(r) = \begin{cases} \hat{\phi}(r) & \text{first branch,} \\ \Delta\phi - \hat{\phi}(r) & \text{second branch,} \end{cases} \tag{2.11}$$

where

$$\hat{\phi}(r) = \tilde{L} \int_{r_1}^{r} \frac{dr'}{r'^2(\tilde{E}^2 - V')^{1/2}}, \tag{2.12}$$

and where $\Delta\phi = 2\hat{\phi}(r_2)$ is the amount by which ϕ increases in the course of one radial orbit.

Equations (2.10) and (2.12) are not directly suitable for numerical integration, because their integrands diverge at both turning points. To facilitate the numerical integration of the geodesic equations, and also their analytical integration in the limiting cases considered below, it is useful to make the substitution

$$r(\chi) = \frac{pM}{1 + e\cos\chi}. \tag{2.13}$$

The parameter χ ranges from 0 to 2π as r goes from r_1 to r_2 and back to r_1; χ is therefore a single-valued parameter along the orbit.

Substituting Eq. (2.13) into (2.2), and using (2.5) and (2.6) we find

$$\pm(\tilde{E}^2 - V)^{1/2} = e\sin\chi \left[\frac{p-6-2e\cos\chi}{p(p-3-e^2)}\right]^{1/2}, \tag{2.14}$$

where the higher (lower) sign corresponds to the first (second) branch of the radial motion. When we substitute Eqs. (2.13) and (2.14) into (2.10) and (2.12) we find that the factor $e\sin\chi$ in $(\tilde{E}^2 - V)^{1/2}$ cancels the same factor in $dr/d\chi$, so that the integrands are now regular. We obtain

$$\begin{aligned} t(\chi) = {} & p^2 M (p-2-2e)^{1/2}(p-2+2e)^{1/2} \\ & \times \int_0^{\chi} d\chi' \, (p-2-2e\cos\chi')^{-1}(1+e\cos\chi')^{-2} \\ & \times (p-6-2e\cos\chi')^{-1/2} \end{aligned} \tag{2.15}$$

and

$$\phi(\chi) = p^{1/2} \int_0^{\chi} \frac{d\chi'}{(p-6-2e\cos\chi')^{1/2}}. \tag{2.16}$$

Since χ is single-valued along the orbit, our expressions for $t(\chi)$ and $\phi(\chi)$ are valid for both branches of the radial motion. The radial period is then given by $P = t(2\pi) = 2t(\pi)$ and $\Delta\phi = \phi(2\pi) = 2\phi(\pi)$.

The substitution $\chi = 2\psi - \pi$ changes the right-hand side of Eq. (2.16) into an elliptic integral of the first kind. The following convenient expression for $\Delta\phi$ is then obtained:

$$\Delta\phi = 4\left(\frac{p}{p-6+2e}\right)^{1/2} K\left(\frac{4e}{p-6+2e}\right), \tag{2.17}$$

where $K(m) = \int_0^{\pi/2} d\psi\,(1-m\sin^2\psi)^{-1/2}$ is the complete elliptic integral of the first kind [31].

D. Fundamental frequencies: Ω_r and Ω_ϕ

Equation (2.17) implies that in general, $\Delta\phi$ is not equal to a rational fraction of 2π. This, in turn, implies that the bound orbits of the Schwarzschild spacetime are not closed. A consequence of this fact is that the motion as a whole, as seen by static observers at infinity, is not periodic in t. Only the radial motion shows a periodicity; the azimuthal motion does not.

The purpose of this subsection is to show that there exists a reference frame in which the motion *is*, after all, periodic. This reference frame rotates with a constant angular velocity Ω_ϕ with respect to the static observers at infinity.

It is clear that $r(t)$ is a periodic function of time, with period P, and that any function of $r(t)$ is also a periodic function of time. Any such periodic function, say $a(t)$, can be decomposed into a Fourier series of the form $a(t) = \sum_k a_k \exp(-ik\Omega_r t)$. Here, the sum is over all integers k, $a_k = P^{-1}\int_0^P dt\, a(t)\exp(ik\Omega_r t)$, and Ω_r is the *radial frequency*:

$$\Omega_r = \frac{2\pi}{P}. \tag{2.18}$$

In particular, the function $a(t) = d\phi/dt$ can be so decomposed, and $\phi(t)$ can then be obtained by integrating the series representation of $a(t)$. The result is $\phi(t) = a_0 t + \sum_k b_k \exp(-ik\Omega_r t)$, where $b_k = ia_k/k\Omega_r$ if $k \neq 0$; b_0 can be determined from the constraint $\sum_k b_k = 0$ which enforces the initial condition $\phi(0) = 0$.

We now see that $\phi(t) - a_0 t$ can be expressed as a Fourier series, and must therefore be a periodic function of time. Clearly, $\phi(t) - a_0 t$ is equal to the angular position of the particle, as determined by an observer rotating with constant angular velocity a_0 with respect to static observers at infinity. As seen by this observer, both radial and azimuthal motions are periodic in t.

Finally, the angular velocity $\Omega_\phi \equiv a_0$ can be calculated to be $P^{-1}\int_0^P dt\, a(t) = \Delta\phi/P$, since $a(t) = d\phi/dt$. The *azimuthal frequency* is therefore given by

$$\Omega_\phi = \frac{\Delta\phi}{2\pi}\,\Omega_r. \tag{2.19}$$

We may conclude that both $r(t)$ and $\phi(t) - \Omega_\phi t$ are periodic functions of time, with a single period P.

E. Orbits near the separatrix: $p \to 6 + 2e$

In this and the following subsections we shall consider two special cases of bound orbits, and derive corresponding expressions for P, $\Delta\phi$, and Ω_ϕ. We begin with the limiting case of orbits lying very close to the separatrix.

We first define the small parameter

$$\varepsilon \equiv p - 6 - 2e, \tag{2.20}$$

whose magnitude will be constrained below. Substituting this into Eqs. (2.15) and (2.17) we obtain

$$P = 16M(1+e)^{1/2}(3+e)^2\left[1+O(\varepsilon)\right] \times \int_0^\pi d\chi\, \frac{A(1-\cos\chi)}{\left[\varepsilon + 2e(1-\cos\chi)\right]^{1/2}}, \tag{2.21}$$

where $A(x) = (2+ex)^{-1}(1+e-ex)^{-2}$, and

$$\Delta\phi = 4\left(\frac{6+2e}{4e+\varepsilon}\right)^{1/2}\left[1+O(\varepsilon)\right]K\left(\frac{4e}{4e+\varepsilon}\right). \tag{2.22}$$

These expressions hold whenever ε is much smaller than unity.

To make our expressions for P and $\Delta\phi$ more explicit, we demand that

$$\varepsilon \ll 4e. \tag{2.23}$$

The alternative requirement, $4e \ll \varepsilon$, will be considered in the next subsection.

Equation (2.23) implies that the argument of the complete elliptic integral in Eq. (2.22) is very close to unity. Using the expansion [31]

$$K(m) = \frac{1}{2}\left[1+O(1-m)\right]\ln\frac{16}{1-m}, \tag{2.24}$$

we arrive at

$$\Delta\phi = 2\left(\frac{3+e}{2e}\right)^{1/2}\left[1+O\left(\frac{\varepsilon}{4e}\right)\right]\ln\frac{64e}{\varepsilon}. \tag{2.25}$$

For bound orbits which are very close to the separatrix, ϕ increases by an amount much larger than 2π in the course of one radial orbit. The particle therefore revolves many times around the central mass before returning to its apastron.

We now manipulate Eq. (2.21) in order to obtain a more manageable expression for P, in the limit $\varepsilon \ll 4e$. The final answer is given in Eq. (2.29) below.

The integrand of Eq. (2.21) diverges at $\chi = 0$ when $\varepsilon = 0$. This corresponds to the fact that when $\varepsilon = 0$, the particle spends an infinite time at $r = r_1$. We shall rewrite Eq. (2.21) so as to isolate this divergent piece of the integral.

The integrand of Eq. (2.21) also diverges at $\chi = \pi$ when $e = 1$. This corresponds to the fact that when $e = 1$, $r_2 = \infty$ and the orbit is no longer bounded. We will also isolate this divergent piece of the integral, so that the remaining piece will be manifestly finite for all values of the orbital parameters.

We first take care of the piece of P which diverges as $\varepsilon \to 0$. For this purpose, we write $A(x) = A(0)[1 + B(x)]$, where $A(1-\cos\chi)$ was defined in Eq. (2.21). The contribution to P which involves $A(0) = (1/2)(1+e)^{-2}$ is divergent, and is proportional to

$$\int_0^\pi \frac{d\chi}{[\varepsilon + 2e(1-\cos\chi)]^{1/2}} = \frac{1}{2e^{1/2}} \ln\frac{64e}{\varepsilon} + O\left(\frac{\varepsilon}{4e}\ln\frac{4e}{\varepsilon}\right); \quad (2.26)$$

we have used Eq. (2.24) to evaluate the integral.

The contribution to P which involves $B(1-\cos\chi)$ is finite as ε tends to zero. Moreover, it can be checked that setting ε to zero in this term only introduces a discrepancy of order $(\varepsilon/4e)\ln 4e/\varepsilon$ which can be absorbed into the second term to the right-hand side of Eq. (2.26). We therefore have to evaluate

$$\int_0^\pi d\chi \frac{B(1-\cos\chi)}{(1-\cos\chi)^{1/2}} \equiv e\int_0^\pi d\chi \frac{C(\cos\chi)}{(1+e\cos\chi)^2}, \quad (2.27)$$

where $C(x) = (3+2e-e^2x^2)(1-x)^{1/2}/(2+e-ex)$.

The integral to the right-hand side of Eq. (2.27) diverges when $e = 1$. To isolate the divergent piece of this integral, we write $C(x) = C(-1) + C'(-1)(1+x) + 2^{-1/2}D(x)$, where a prime denotes differentiation with respect to the argument. The contributions to the integral involving $C(-1) = 2^{-1/2}(3-e)$ and $C'(-1) = 2^{-5/2}(7e-3)$ both diverge when $e = 1$, because $\int_0^\pi d\chi\,(1+e\cos\chi)^{-2} = \pi(1-e^2)^{-3/2}$ and $\int_0^\pi d\chi\,(1+\cos\chi)(1+e\cos\chi)^{-2} = \pi(1+e)^{-1}(1-e^2)^{-1/2}$. On the other hand, the contribution involving

$$D(\cos\chi) = \frac{3+2e-e^2\cos^2\chi}{2+e(1-\cos\chi)}[2(1-\cos\chi)]^{1/2} - 3 + e - \tfrac{1}{4}(7e-3)(1+\cos\chi) \quad (2.28)$$

is finite.

Gathering the results, we find that the orbital period can be expressed as

$$P = 4Me^{-1/2}(1+e)^{-3/2}(3+e)^2 \times \left[\ln\frac{64e}{\varepsilon} + \frac{\pi e(9+6e-7e^2)}{4(1-e^2)^{3/2}} + eI(e) + O\left(\frac{\varepsilon}{4e}\ln\frac{4e}{\varepsilon}\right)\right], \quad (2.29)$$

where $I(e) = \int_0^\pi d\chi\,(1+e\cos\chi)^{-2}D(\cos\chi)$ is finite for any e. This integral can be evaluated numerically, and we find that $I(e)$ lies within the range $-2.1149 \simeq I(1) \le I(e) \le I(0) = 6 - 9\pi/4 \simeq -1.0686$.

We now derive an approximate expression for Ω_ϕ. For convenience, we assume that ε is chosen small enough that in Eq. (2.29), the first term within the square brackets always dominates. We therefore demand that when $e \to 1$,

$$\varepsilon \ll 4e\exp[-(1-e^2)^{-3/2}]. \quad (2.30)$$

When Eqs. (2.23) and (2.30) hold,

$$\beta \equiv \left[\frac{\pi e(9+6e-7e^2)}{4(1-e^2)^{3/2}} + eI(e)\right]\left(\ln\frac{64e}{\varepsilon}\right)^{-1} \quad (2.31)$$

is always much smaller than unity.

Using Eqs. (2.18), (2.19), (2.25), (2.29), and (2.31) we find that the azimuthal frequency is given by

$$M\Omega_\phi = \left(\frac{1+e}{6+2e}\right)^{3/2}\left[1-\beta+O\left(\frac{\varepsilon}{4e}\right)\right], \quad (2.32)$$

whenever ε satisfies the inequalities (2.23) and (2.30); and when these hold, $\beta = O(2\pi/\Delta\phi) = O[(\ln 4e/\varepsilon)^{-1}] \gg O(\varepsilon/4e)$.

F. Slightly eccentric orbits: $e \to 0$

It is much easier to derive expressions for P, $\Delta\phi$, and Ω_ϕ for the limiting case of slightly eccentric orbits. We now demand that

$$e \ll \min(1, p-6), \quad (2.33)$$

which we shall impose throughout this subsection.

It is a straightforward matter to use the expansion [31]

$$K(m) = \frac{\pi}{2}\left[1 + \tfrac{1}{4}m + \tfrac{9}{64}m^2 + \tfrac{225}{2304}m^3 + O(m^4)\right] \quad (2.34)$$

so as to express Eq. (2.17) as a power series in e. We find

$$\Delta\phi = 2\pi\left(\frac{p}{p-6}\right)^{1/2}\left[1 + \frac{3}{4(p-6)^2}e^2 + O(e^4)\right]. \quad (2.35)$$

Similarly, we may expand Eq. (2.15) in powers of the eccentricity, and then integrate term by term. We obtain

$$P = \frac{2\pi Mp^2}{(p-6)^{1/2}}\left[1 + \frac{3(2p^3-32p^2+165p-266)}{4(p-2)(p-6)^2}e^2 + O(e^4)\right]. \quad (2.36)$$

Finally, by combining Eqs. (2.18), (2.19), (2.35), and (2.36) we arrive at

$$M\Omega_\phi = p^{-3/2}\left[1 - \frac{3(p^2-10p+22)}{2(p-2)(p-6)}e^2 + O(e^4)\right]. \quad (2.37)$$

In Eqs. (2.35)–(2.37), the symbol $O(e^4)$ is used to represent those terms which are fourth or higher order in the eccentricity; these include terms proportional to $e^4/(p-6)^4$. The limit $p \to 6$ must therefore be taken with care, always ensuring that $e \ll p-6$.

III. RADIATION REACTION

In this section we present our method for calculating the effects of radiation reaction on the bound orbits of the Schwarzschild spacetime. The method is based upon the Teukolsky formalism for black-hole perturbations [20], which is reviewed below. A more detailed presentation can be found in Refs. [1,32].

A. The method

Our strategy for calculating the evolution, under radiation reaction, of the bound orbits of the Schwarzschild spacetime was presented in Sec. I C. In short:

We begin by assuming that the motion of the particle is geodesic over a time scale comparable to the orbital period. The validity of this assumption follows from the adiabatic approximation, which states that radiation reaction operates over a much longer time scale.

We use the Teukolsky formalism to calculate $\dot{E}$ and $\dot{L}$, respectively, the time-averaged rates at which the gravitational waves carry away energy and angular momentum. The waves are generated by the orbiting particle, and the average is taken over several orbital periods.

We assume that the orbital parameters change according to

$$\left\langle \frac{d\tilde{E}}{dt} \right\rangle = -\mu\dot{E}, \qquad \left\langle \frac{d\tilde{L}}{dt} \right\rangle = -\mu\dot{L}, \tag{3.1}$$

so that the total energy of the whole system (black hole plus particle plus waves) is conserved. The symbol $\langle\ \rangle$ designates the time average.

Because of the radiation reaction, the particle's world line is not strictly a geodesic. However, as required by the adiabatic approximation, and in agreement with our initial assumption, the deviations from geodesic motion become noticeable only after a large number of orbits.

The only essential assumption made in this calculation is that μ/M is sufficiently small that (i) the gravitational perturbations obey linear wave equations and (ii) the adiabatic approximation is valid. In Sec. IV D we shall formulate precise conditions on μ/M which ensure the validity of the adiabatic approximation.

B. The Teukolsky formalism

In the Teukolsky formalism, gravitational perturbations are described by the Weyl scalar $\Psi_4 = -C_{\alpha\beta\gamma\delta}n^\alpha\bar{m}^\beta n^\gamma\bar{m}^\delta$, where $C_{\alpha\beta\gamma\delta}$ is the Weyl tensor, $n^\alpha = \frac{1}{2}(1,-f,0,0)$, and $\bar{m}^\alpha = (0,0,1,-i\csc\theta)/\sqrt{2}r$. Throughout we denote complex conjugation with an overbar. At large distances, Ψ_4 describes outgoing gravitational waves.

The Weyl scalar can be decomposed into Fourier-harmonic components according to

$$\Psi_4 = \int_{-\infty}^{\infty} d\omega \sum_{\ell m} r^{-4} R_{\omega\ell m}(r)\,{}_{-2}Y_{\ell m}(\theta,\phi)e^{-i\omega t}, \tag{3.2}$$

where ${}_sY_{\ell m}(\theta,\phi)$ are spin-weighted spherical harmonics [33]. The sums over ℓ and m are restricted to $-\ell \le m \le \ell$ and $\ell \ge 2$. The radial function $R_{\omega\ell m}(r)$ satisfies the inhomogeneous Teukolsky equation

$$\left[r^2 f\frac{d^2}{dr^2} - 2(r-M)\frac{d}{dr} + U(r)\right]R_{\omega\ell m}(r) = -T_{\omega\ell m}(r), \tag{3.3}$$

with

$$U(r) = f^{-1}\left[(\omega r)^2 - 4i\omega(r-3M)\right] - \lambda, \tag{3.4}$$

where $\lambda = (\ell-1)(\ell+2)$.

The source term in Eq. (3.3) is calculated from the particle's stress-energy tensor,

$$T^{\alpha\beta}(x) = \mu\int d\tau\, u^\alpha u^\beta \delta^{(4)}\left[x - x'(\tau)\right], \tag{3.5}$$

where x is the spacetime point, $x'(\tau)$ the particle's world line with tangent vector $u^\alpha = dx'^\alpha/d\tau$, and τ denotes proper time. The first step is to construct the projections ${}_0T = T_{\alpha\beta}n^\alpha n^\beta$, ${}_{-1}T = T_{\alpha\beta}n^\alpha\bar{m}^\beta$, and ${}_{-2}T = T_{\alpha\beta}\bar{m}^\alpha\bar{m}^\beta$. Then one calculates the Fourier-harmonic components ${}_sT_{\omega\ell m}(r)$ according to

$${}_sT_{\omega\ell m}(r) = \frac{1}{2\pi}\int dt\, d\Omega\, {}_sT\, {}_s\bar{Y}_{\ell m}(\theta,\phi)e^{i\omega t}, \tag{3.6}$$

where $d\Omega$ is the element of solid angle. Finally, the source is [32,34]

$$\begin{aligned} T_{\omega\ell m}(r) = 2\pi\Big\{ & 2\left[\lambda(\lambda+2)\right]^{1/2} r^4\, {}_0T_{\omega\ell m}(r) \\ & + 2(2\lambda)^{1/2} r^2 f\mathcal{L}\, r^3 f^{-1}\, {}_{-1}T_{\omega\ell m}(r) \\ & + rf\mathcal{L}r^4 f^{-1}\mathcal{L}\, r\, {}_{-2}T_{\omega\ell m}(r)\Big\}, \end{aligned} \tag{3.7}$$

where $\mathcal{L} = f d/dr + i\omega$.

The inhomogeneous Teukolsky equation (3.3) can be integrated by means of a Green's function [35]. (The Green's function is so constructed that Ψ_4 satisfies a no-incoming-radiation condition.) The solution at large radii is

$$R_{\omega\ell m}(r\to\infty) \sim \mu\omega^2 Z_{\omega\ell m} r^3 e^{i\omega r^*}, \tag{3.8}$$

and represents purely outgoing waves. Here, $r^* = r + 2M\ln(r/2M-1)$. The amplitudes $Z_{\omega\ell m}$ are given by

$$Z_{\omega\ell m} = \frac{1}{2i\mu\omega^2 Q^{\rm in}_{\omega\ell}}\int_{2M}^{\infty} dr\, \frac{R^H_{\omega\ell}(r)T_{\omega\ell m}(r)}{r^4 f^2}, \tag{3.9}$$

where the function $R^H_{\omega\ell}(r)$ is the solution to the *homogeneous* Teukolsky equation with ingoing-wave boundary conditions at the black-hole horizon: $R^H_{\omega\ell}(r\to 2M) \sim (\omega r)^4 f^2 e^{-i\omega r^*}$. At infinity, $R^H_{\omega\ell}(r)$ represents a superpostion of ingoing and outgoing waves, $R^H_{\omega\ell}(r\to\infty) \sim Q^{\rm in}_{\omega\ell}(\omega r)^{-1}e^{-i\omega r^*} + Q^{\rm out}_{\omega\ell}(\omega r)^3 e^{i\omega r^*}$; $Q^{\rm in}_{\omega\ell}$ and $Q^{\rm out}_{\omega\ell}$ are constants, independent of r. The amplitudes $Z_{\omega\ell m}$ satisfy the identities

$$\bar{Z}_{-\omega,\ell,-m} = (-1)^\ell Z_{\omega\ell m}, \tag{3.10}$$

which are derived in Ref. [1].

We now specialize to the case considered in this paper, for which the frequency spectrum of the perturbations contains only a discrete set of distinct frequencies ω_{mk} (Sec. III C). We then have

$$Z_{\omega\ell m} = \sum_k Z^k_{\ell m}\delta(\omega - \omega_{mk}). \tag{3.11}$$

As indicated, the frequencies ω_{mk} are characterized by two sets of integers, m and k. The time-averaged rates at

which the gravitational waves carry energy and angular momentum to infinity are calculated to be

$$\dot{E}^{\infty} = \sum_{\ell m k} \dot{E}^{\infty}_{\ell m k}, \qquad \dot{L}^{\infty} = \sum_{\ell m k} \dot{L}^{\infty}_{\ell m k}, \tag{3.12}$$

where

$$\dot{E}^{\infty}_{\ell m k} = \frac{\mu^2}{4\pi}\, {\omega_{mk}}^2 |Z^k_{\ell m}|^2, \tag{3.13}$$

and

$$\dot{L}^{\infty}_{\ell m k} = \frac{\mu^2}{4\pi}\, m\omega_{mk} |Z^k_{\ell m}|^2. \tag{3.14}$$

We stress that $\dot{E}^{\infty}$ and $\dot{L}^{\infty}$ represent *time-averaged* rates; the average is taken over several orbital periods. For reasons to be given in Sec. V E, we will not consider here the energy and angular momentum which are absorbed by the black hole. To an accuracy sufficient for our purposes, we shall neglect these contributions to $\dot{E}$ and $\dot{L}$, and set $\dot{E} = \dot{E}^{\infty}$, $\dot{L} = \dot{L}^{\infty}$.

C. Calculation of ${}_sT_{\omega\ell m}(r)$

We now proceed with the calculation of the source term in Eq. (3.3), taking the particle's world line to be a bound geodesic of the Schwarzschild spacetime. Our starting point is the particle's stress-energy tensor, which is given by Eq. (3.5). After integration, this becomes

$$T^{\alpha\beta}(x) = \mu \frac{u^\alpha u^\beta}{r'^2 u^t} \delta(r - r') \delta(\cos\theta) \delta(\phi - \phi'). \tag{3.15}$$

Here, $\{t, r, \theta, \phi\}$ are the coordinates of the spacetime point x, and $\{t, r'(t), \pi/2, \phi'(t)\}$ describe the particle's world line; the four-velocity $u^\alpha = dx'^\alpha/d\tau$ can be obtained from Eq. (2.1).

Following the procedure given in Sec. III B we find

$${}_sT_{\omega\ell m}(r) = \frac{\mu}{2\pi}\, {}_sY_{\ell m}(\tfrac{\pi}{2}, 0) \times \int_{-\infty}^{\infty} dt\, {}_sF(r') \delta(r - r') e^{i(\omega t - m\phi')}, \tag{3.16}$$

where

$${}_sF(r') = \frac{1}{r'^2 u^t} \begin{cases} (u\cdot n)^2 & s = 0, \\ (u\cdot n)(u\cdot \bar{m}) & s = -1, \\ (u\cdot \bar{m})^2 & s = -2. \end{cases} \tag{3.17}$$

Here, $u \cdot n \equiv u^\alpha n_\alpha$, etc., and the vectors n^α and $\bar{m}^\alpha$ are evaluated on the particle's world line.

To evaluate the integral of Eq. (3.16), we rewrite the integrand as ${}_sa(t) \exp[i(\omega - m\Omega_\phi)t]$, where ${}_sa(t) = {}_sF(r')\delta(r - r') \exp[-im(\phi' - \Omega_\phi t)]$. According to the results of Sec. II D, the functions ${}_sa(t)$ are periodic in t, with period P. This means that we can express these functions as Fourier series of the form $\sum_k {}_sa_k \exp(-ik\Omega_r t)$, with ${}_sa_k = P^{-1}\int_0^P {}_sa(t) \exp(ik\Omega_r t)$. We then substitute the series representations of ${}_sa(t)$ into Eq. (3.16), which is now easily integrated. The result is

$${}_sT_{\omega\ell m}(r) = \mu\, {}_sY_{\ell m}(\tfrac{\pi}{2}, 0) P^{-1} \sum_k \delta(\omega - \omega_{mk}) \times \int_0^P dt\, {}_sF(r') \delta(r - r') e^{i(\omega_{mk} t - m\phi')}. \tag{3.18}$$

The frequency spectrum is given by

$$\omega_{mk} = m\Omega_\phi + k\Omega_r, \tag{3.19}$$

where k is an integer running from $-\infty$ to $+\infty$. Equations (3.18) and (3.19) express the fact that the frequency spectrum contains only a discrete set of distinct frequencies, the harmonics of the fundamental frequencies Ω_ϕ and Ω_r. This fact has already been used in Eq. (3.11) above.

We now transform Eq. (3.18) into an integral over r', using $dr'/dt = \pm f' \tilde{E}^{-1} (\tilde{E}^2 - V')^{1/2}$, where the higher (lower) sign refers to the first (second) branch of the radial motion (Sec. II C); we also have $f' = 1 - 2M/r'$ and $V' = V(\tilde{L}, r')$. Breaking the integration into two parts corresponding to each branch, we find that Eq. (3.18) becomes

$$\begin{aligned} {}_sT_{\omega\ell m}(r) = \mu\, {}_sY_{\ell m}(\tfrac{\pi}{2}, 0) &\Theta(r - r_1)\Theta(r_2 - r) \\ &\times f^2 P^{-1} (\tilde{E}^2 - V)^{-1/2} \sum_k \delta(\omega - \omega_{mk}) \\ &\times \sum_{\pm} {}_sG_{\pm}(r) e^{\pm i[\omega_{mk} \hat{t}(r) - m\hat{\phi}(r)]}. \end{aligned} \tag{3.20}$$

Here, $\Theta(r)$ is the Heaviside step function, $f = 1 - 2M/r$, $V = V(\tilde{L}, r)$; $\hat{t}(r)$ and $\hat{\phi}(r)$ were defined in Eqs. (2.10) and (2.12). We also have ${}_sG_{\pm} = \tilde{E}\, {}_sF/f^3$, where the right-hand side is evaluated on the first (higher sign), or second (lower sign), branch of the radial motion. More explicitly, making use of Eq. (3.17),

$${}_sG_{\pm}(r) = \frac{1}{4r^4 f^2} \begin{cases} r^2[\tilde{E} \pm (\tilde{E}^2 - V)^{1/2}]^2 & s = 0, \\ \sqrt{2} i r \tilde{L} [\tilde{E} \pm (\tilde{E}^2 - V)^{1/2}] & s = -1, \\ -2\tilde{L}^2 & s = -2. \end{cases} \tag{3.21}$$

D. Calculation of $Z^k_{\ell m}$

In this subsection we calculate the amplitudes $Z^k_{\ell m}$ using Eqs. (3.7), (3.9), (3.11), and (3.20). These can then be substituted into Eqs. (3.13) and (3.14) to calculate the contributions to $\dot{E}$ and $\dot{L}$ from each ℓ, m, and k. The final result is obtained by summing over all these integers, as shown in Eq. (3.12)

We start from Eq. (3.7), which we reexpress as $T_{\omega\ell m} = 2\pi \sum_s {}_sD_{\omega\ell}\, {}_sT_{\omega\ell m}$, where the operators ${}_sD_{\omega\ell}$ can easily be identified. For convenience, we also rewrite Eq. (3.9) as

$$Z_{\omega\ell m} = \left(2i\mu\omega^2 Q^{\rm in}_{\omega\ell}\right)^{-1} \sum_s {}_sZ_{\omega\ell m}, \tag{3.22}$$

where

$$ {}_sZ_{\omega\ell m} = 2\pi \int_{2M}^{\infty} dr\, \frac{R^H_{\omega\ell}(r)\, {}_sD_{\omega\ell}\, {}_sT_{\omega\ell m}(r)}{r^4 f^2}. \tag{3.23} $$

The right-hand side of Eq. (3.23) can be regarded as an inner product (R, DT), where R and T are functions, and D an operator (we have suppressed the use of the indices for greater clarity). To simplify the evaluation of this inner product, we define the adjoint operator $D^\dagger$ such that $(R, DT) = (D^\dagger R, T)$. This new operator can be calculated by performing a number of integration by parts on Eq. (3.23). After such manipulations, we find that Eq. (3.23) becomes

$$ {}_sZ_{\omega\ell m} = 2\pi\, {}_sp_\ell \int_{2M}^{\infty} dr\, f^{-2}\, {}_sR^H_{\omega\ell}(r)\, {}_sT_{\omega\ell m}(r). \tag{3.24} $$

We have introduced

$$ {}_sp_\ell = \begin{cases} 2\left[\lambda(\lambda+2)\right]^{1/2} & s = 0, \\ 2(2\lambda)^{1/2} & s = -1, \\ 1 & s = -2, \end{cases} \tag{3.25} $$

where $\lambda = (\ell-1)(\ell+2)$, together with

$$ {}_0R^H_{\omega\ell}(r) = R^H_{\omega\ell}(r), \tag{3.26} $$

$$ {}_{-1}R^H_{\omega\ell}(r) = \left(-rf\frac{d}{dr} + 2f + i\omega r\right) R^H_{\omega\ell}(r), \tag{3.27} $$

$$ {}_{-2}R^H_{\omega\ell}(r) = \left[r^2 f^2 \frac{d^2}{dr^2} - 2rf(f + i\omega r)\frac{d}{dr} + i\omega r(2 - 2M/r + i\omega r)\right] R^H_{\omega\ell}(r). \tag{3.28} $$

Equations (3.24)–(3.28) are valid irrespective of the choice of source functions ${}_sT_{\omega\ell m}(r)$.

The final step is to specialize to the source functions which are relevant to our problem, and to substitute Eq. (3.20) into (3.24). Using Eqs. (3.11) and (3.22) along the way, we find

$$ Z^k_{\ell m} = \left[2i\mu(\omega_{mk})^2 Q^{\rm in}_{\omega_{mk}\ell}\right]^{-1} \sum_s {}_sZ^k_{\ell m}, \tag{3.29} $$

with

$$ {}_sZ^k_{\ell m} = \mu\, {}_sp_\ell\, {}_sY_{\ell m}(\tfrac{\pi}{2}, 0)\Omega_r \sum_{\pm} \int_{r_1}^{r_2} dr\, (\tilde{E}^2 - V)^{-1/2} \times {}_sG_{\pm}(r)\, {}_sR^H_{\omega_{mk}\ell}(r) e^{\pm i[\omega_{mk}\hat{t}(r) - m\hat{\phi}(r)]}. \tag{3.30} $$

In general, the integrals of Eq. (3.30) must be evaluated numerically. To facilitate these integrations, we make the substitution $r = r(\chi)$, given in Eq. (2.13), which removes the bad behavior of the integrand at $r = r_1$ and $r = r_2$. This change of variables also makes the perturbation formalism robust, in the sense that the limit $e = 0$ can be taken directly, without difficulty.

E. The radiation-reaction equations

The Teukolsky formalism, as summarized in the preceding subsections, allows us to calculate $\dot{E}$ and $\dot{L}$, the time-averaged rates at which the gravitational waves carry away energy and angular momentum. Using Eq. (3.1), we can then infer the time-averaged rates of change of the orbital parameters.

In Sec. II B we have introduced the quantities p and e as a preferred set of orbital parameters. The purpose of this subsection is to relate the rates of change of p and e to $\dot{E}$ and $\dot{L}$, which are directly obtained from the Teukolsky formalism.

Since p and e are functions of $\tilde{E}$ and $\tilde{L}$, we have, using Eq. (3.1), $-\dot{E} = (\partial\tilde{E}/\partial p)\mu\dot{p} + (\partial\tilde{E}/\partial e)\mu\dot{e}$ and $-\dot{L} = (\partial\tilde{L}/\partial p)\mu\dot{p} + (\partial\tilde{L}/\partial e)\mu\dot{e}$. These equations can easily be inverted. Using Eqs. (2.5) and (2.6), we find

$$ \mu\dot{p} = \frac{2(p - 3 - e^2)^{1/2}}{(p - 6 - 2e)(p - 6 + 2e)} \Big[p^{3/2}(p - 2 - 2e)^{1/2} \times (p - 2 + 2e)^{1/2}\dot{E} - (p-4)^2\dot{L}/M\Big] \tag{3.31} $$

and

$$ \mu\dot{e} = \frac{(p - 3 - e^2)^{1/2}}{ep(p - 6 - 2e)(p - 6 + 2e)} \Big\{-p^{3/2}(p - 6 - 2e^2) \times (p - 2 - 2e)^{1/2}(p - 2 + 2e)^{1/2}\dot{E} + (1 - e^2)\left[(p-2)(p-6) + 4e^2\right]\dot{L}/M\Big\}. \tag{3.32} $$

It is important to notice that Eqs. (3.31) and (3.32) are singular at $p = 6 + 2e$.

Radiation reaction produces a slow evolution of the orbital parameters, and therefore generates curves in the p-e plane. We can anticipate that the curves must all cross the separatrix $p = 6 + 2e$, so that the particle must eventually plunge inside the black hole. To see this, we only need recall that the gravitational waves remove angular momentum from the system. This induces a decrease in $V_{\rm max}$, the value of the effective potential at the local maximum (see Fig. 4). When $\tilde{L}$ reaches the critical value $2\sqrt{3}M$, the potential barrier disappears altogether. The particle must therefore plunge either at, or prior to, this point. In the former case (plunging when $\tilde{L} = 2\sqrt{3}M$), the particle's orbit is circular immediately before plunging; in the latter (plunging when $\tilde{L} > 2\sqrt{3}M$), the orbit is eccentric.

The detailed behavior of the radiation-reaction curves near $p = 6 + 2e$ will be discussed in Sec. IV B.

IV. ANALYTICAL RESULTS

The first part of this section (Sec. IV A–C) is devoted to the calculation of the radiation-reaction curves (Sec. III E) in those regions of the p-e plane for which the calculation can be performed, to some degree of accuracy, analytically. More specifically, we shall be interested in evaluating $\dot{p}$ and $\dot{e}$, as well as the function

$$ c(p, e) = \frac{d\ln e}{d\ln p}. \tag{4.1} $$

In Eq. (4.1), the variations in p and e are calculated using the radiation-reaction equations (3.31) and (3.32). Notice also that dp and de denote time-averaged variations;

as usual, the average is taken over several orbital periods.

In the second part of this section (Sec. IV D), we will use our analytical expressions for $\dot{p}$ and $\dot{e}$ to formulate constraints on the magnitude of μ/M. These will ensure the validity of the adiabatic approximation (Sec. III A) throughout the p-e plane.

A. Weak-field radiation reaction: $p \gg 6$

The effects of gravitational radiation reaction in weak-field, slow-motion situations are well understood and can be derived, to leading order [11], using a Newtonian potential of the form $\Phi_{\rm rr} = (1/5)(d^5 Q_{ab}/dt^5)x^a x^b$, where Q_{ab} is the traceless quadrupole moment of the mass distribution [4–7]. The radiation-reaction force is then given by $\boldsymbol{F}_{\rm rr} = -\mu\nabla\Phi_{\rm rr}$, and the resulting equations of motion can be used to calculate the rates of change of the orbital parameters.

We shall instead follow the equivalent procedure of using the $p \to \infty$ limit of Eqs. (3.31) and (3.32), together with suitable expressions for $\dot{E}$ and $\dot{L}$, to calculate $\dot{p}$ and $\dot{e}$. The equations of Sec. III could be integrated analytically in the limit $p \to \infty$, so as to yield the desired expressions for the fluxes of energy and angular momentum. (See Refs. [32,36,37] for similar analytical integrations of the perturbation equations.) However, it is much easier to obtain $\dot{E}$ and $\dot{L}$ from Peters' classic paper [21], in which they are calculated, to leading order in the weak-field limit, using the quadrupole formulas [5]. The results are

$$\dot{E} = \frac{32}{5}\left(\frac{\mu}{M}\right)^2 p^{-5}\left(1-e^2\right)^{3/2}\left(1+\tfrac{73}{24}e^2+\tfrac{37}{96}e^4\right) \quad (4.2)$$

and

$$\dot{L}/M = \frac{32}{5}\left(\frac{\mu}{M}\right)^2 p^{-7/2}\left(1-e^2\right)^{3/2}\left(1+\tfrac{7}{8}e^2\right). \quad (4.3)$$

Equations (4.2) and (4.3) are valid up to fractional corrections of order p^{-1}.

It is then a matter of simple algebra to substitute Eqs. (4.2) and (4.3) into the $p \to \infty$ limit of (3.31) and (3.32) to obtain

$$\mu\dot{p} = -\frac{64}{5}\left(\frac{\mu}{M}\right)^2 p^{-3}\left(1-e^2\right)^{3/2}\left(1+\tfrac{7}{8}e^2\right) \quad (4.4)$$

and

$$\mu\dot{e} = -\frac{304}{15}\left(\frac{\mu}{M}\right)^2 p^{-4}e\left(1-e^2\right)^{3/2}\left(1+\tfrac{121}{304}e^2\right). \quad (4.5)$$

These equations imply that weak-field radiation reaction decreases *both* the semi-latus rectum p and the eccentricity e.

Substituting Eqs. (4.4) and (4.5) into (4.1) we arrive at

$$c(p,e) = \tfrac{19}{12}\left[1+O\left(p^{-1}\right)\right]\left(1+\tfrac{7}{8}e^2\right)^{-1}\left(1+\tfrac{121}{304}e^2\right), \quad (4.6)$$

which is valid for large p and any value of e.

Equation (4.6) implies the well-known result that an initially eccentric orbit becomes circular if radiation reaction operates for a sufficiently long time [21,22]. (This conclusion, we stress, is only true for weak-field radiation reaction.)

It is worth noting that the results presented in this subsection are valid also for binary systems with arbitrary mass ratios [21], provided that μ is then interpreted as the reduced mass of the system, M as the total mass, and p and e as the orbital parameters of the *relative* orbit.

B. Strong-field radiation reaction: $p - 6 - 2e \ll 4e$

The region of the p-e plane which lies very close to the separatrix $p = 6 + 2e$ is also amenable to approximate, analytical calculations. In this subsection we will take $\varepsilon/4e$, where

$$\varepsilon \equiv p - 6 - 2e, \quad (4.7)$$

to be much smaller than unity.

Our starting point is the statement that when $p = 6 + 2e$, so that the orbit is circular and unstable (Sec. II B), the fluxes of energy and angular momentum are related by $\dot{E} = \Omega_\phi \dot{L}$, where Ω_ϕ is given by the $\varepsilon = 0$ limit of Eq. (2.32): $M\Omega_\phi = (1+e)^{3/2}/(6+2e)^{3/2}$. This statement can be justified as follows. Equation (2.29) implies that the radial period P diverges when ε approaches zero, which means that $\Omega_r = 2\pi/P$ vanishes in that limit. From Eq. (3.19) we then find that the frequency spectrum of the gravitational perturbations is given by $\omega_{mk} = m\Omega_\phi$. Finally, substituting this into Eqs. (3.12)–(3.14) shows that the fluxes of energy and angular momentum *at infinity* satisfy the equality $\dot{E} = \Omega_\phi \dot{L}$. It can also be shown that this frequency spectrum implies the same relationship between the fluxes at the black-hole horizon. (For explicit expressions see Ref. [1].) The desired result therefore follows.

The transformation $\{\dot{E}, \dot{L}\} \to \{\dot{p}, \dot{e}\}$ is singular at $\varepsilon = 0$; see Sec. III E. In order to calculate $\dot{p}$ and $\dot{e}$ in the limit $\varepsilon/4e \ll 1$, we need to know the relationship between $\dot{E}$ and $\dot{L}$ for orbits which are slightly away from the separatrix. The discussion of the previous paragraph allows us to write

$$\dot{E} = (1+\alpha)\Omega_\phi \dot{L}, \qquad \alpha \ll 1, \quad (4.8)$$

where α is only known to vanish in the limit $\varepsilon = 0$. We do not need to know the relative magnitude of α, in relation with ε, for our purposes. However, it may be argued, using Eqs. (2.19) and (2.25), that $\alpha = O(\Omega_r/\Omega_\phi) = O(2\pi/\Delta\phi) = O[(\ln 4e/\varepsilon)^{-1}] \gg O(\varepsilon/4e)$. We will not need to rely on this crude, nonrigorous estimate.

Substituting Eq. (2.32) into (4.8) we arrive at

$$\frac{\dot{L}}{M\dot{E}} = \left(\frac{6+2e}{1+e}\right)^{3/2}\left[1+\beta-\alpha+O\left(\frac{\varepsilon}{4e}\right)\right]. \quad (4.9)$$

We have neglected, in the square brackets, terms of quadratic and higher order in α. In Eq. (4.9), the relative magnitude of α, compared to that of β and $\varepsilon/4e$,

is not precisely known [it is most likely that α and β are of comparable magnitude; see Eq. (2.31)]. However, this information is not needed to calculate $c(e,p)$. What is required for the calculation is the knowledge that $\beta \gg O(\varepsilon/4e)$, so that the term $\beta-\alpha$ is the larger correction term in Eq. (4.9). (We dismiss as improbable the possibility that α and β are equal up to terms of order $\varepsilon/4e$ or smaller. We have verified numerically that $\beta-\alpha$ is always much larger than $\varepsilon/4e$.)

The substitution of Eq. (4.9) into (3.31) and (3.32) yields

$$\mu\dot{p} = -2e^{-1}(1+e)(3-e)^{1/2}(6+2e)^{3/2} \times \frac{\beta-\alpha+O(\varepsilon/4e)}{\varepsilon}\dot{E} \tag{4.10}$$

and

$$\mu\dot{e} = 2e^{-1}(1-e)(1+e)(3-e)^{1/2}(6+2e)^{1/2} \times \frac{\beta-\alpha+O(\varepsilon/4e)}{\varepsilon}\dot{E}. \tag{4.11}$$

Here, $\dot{E}$ is evaluated on the separatrix, where it is finite and nonvanishing. Use of Eq. (4.1) then gives

$$c(p,e) = -\frac{1-e}{e}\left\{1+O\left[\frac{\varepsilon}{4e(\beta-\alpha)}\right]\right\}, \tag{4.12}$$

which is valid for $\varepsilon/4e \ll 1$. According to our previous estimate for the magnitude of α, it is most likely that the correction term in Eq. (4.12) is of order $(\varepsilon/4e)\ln(\varepsilon/4e)$.

Although α cannot be calculated analytically, we may nevertheless state that near the separatrix, $\dot{p}<0$ and $\dot{e}>0$, which implies that $\beta-\alpha+O(\varepsilon/4e)>0$. This statement follows from (i) the fact that $de/dp<0$ near the separatrix, which is a consequence of Eq. (4.12), and (ii) the fact that the radiation-reaction curves must cross the separatrix, a property that was proved in Sec. III E.

We have therefore established that radiation reaction acts on orbits which are close to the separatrix so as to decrease the semi-latus rectum p, and to *increase* the eccentricity e [23]. This is in marked contrast with weak-field radiation reaction, which decreases the eccentricity. We remark that for fixed μ/M, the divergence of $\mu\dot{p}$ and $\mu\dot{e}$ in the limit $\varepsilon\to 0$ signals the breakdown of the adiabatic approximation. This point will be discussed in Sec. IV D.

The asymptotic expressions for $c(e,p)$, Eqs. (4.6) and (4.12), together with the fact that radiation reaction always decreases p, imply the existence of a *critical curve* in the p-e plane, along which $de/dp=0$. Equation (4.12) further implies that the critical curve meets with the separatrix at $e=1$. The existence of such a curve is a genuine strong-field effect, which can perhaps be understood as a precursor effect to the eventual plunging of the orbit. The precise location of the critical curve can be found by numerically integrating the perturbation equations. A portion of the critical curve is displayed in Fig. 3.

C. Strong-field radiation reaction: $e \ll p-6$

The results derived in the preceding subsection are valid for small eccentricities, provided that $p-6-2e$ is always taken to be much smaller than $4e$. This amounts to approaching the point $(p,e)=(6,0)$ along a path which lies very close to the separatrix $p=6+2e$. In this subsection, we calculate $\dot{p}$, $\dot{e}$, and $c(p,e)$ also in the neighborhood of the point $(6,0)$, but now approaching it on a path which lies very close to $e=0$. This amounts to taking the limits $e\to 0$, $p\to 6$ *in that order*, always ensuring that $e/(p-6)\ll 1$. As we shall see, the point $(6,0)$ is a singular point of the p-e plane, in the sense that $c(e,p)$ diverges there, and that its degree of divergence depends on the direction of approach.

The results contained in this subsection are not new, and were first presented in Ref. [1]. We shall nevertheless repeat this analysis here, for two main reasons. First, we wish this paper to be as complete and self-contained as possible, and the case $e \ll p-6$ must be discussed. And second, our rederivation of the results will allow us to formulate an assumption that was left implicit in Ref. [1]; this assumption concerns the order in which the limits $e\to 0$, $p\to 6$ are taken.

Our starting point is the statement that for stable circular orbits, the fluxes of energy and angular momentum are related by $\dot{E}=\Omega_\phi \dot{L}$, where Ω_ϕ is given by the $e=0$ limit of Eq. (2.37): $M\Omega_\phi = p^{-3/2}$. This statement is justified by first taking the $e=0$ limit of Eq. (3.30). [This limit is taken only after the substitution $r=r(\chi)$, Eq. (2.13), is made, and (2.14) used.] The explicit evaluation of ${}_sZ^k_{\ell m}$ is straightforward in that limit. The result is that ${}_sZ^k_{\ell m}$ vanishes unless $k=0$, which implies that the harmonics of the radial frequency Ω_r do not contribute to the frequency spectrum, Eq. (3.19). Finally, use of Eq. (3.29), and then of (3.12)–(3.14), yields the desired result. (Actually, this argument proves only that the fluxes at infinity satisfy the relation $\dot{E}=\Omega_\phi\dot{L}$. However, the argument can be generalized so as to also include the fluxes at the black-hole horizon, for which the same relation holds. This more complete analysis is presented in Ref. [1].)

When the orbit is slightly eccentric, we have that $\dot{E}$ and $\dot{L}$ are now related by

$$\dot{E} = [1+\gamma e^2 + O(e^4)]\Omega_\phi \dot{L}. \tag{4.13}$$

That the first-order correction is quadratic in e can be expected from the results of Sec. II F; this can also be justified rigorously by taking the small-eccentricity limit of the relevant equations of Sec. III. This analysis was carried out in Ref. [1], which also reveals that $\gamma(p)$ is well behaved in the limit $p\to 6$ [38]. This property will be used below.

It is straightforward to substitute Eq. (2.37) into (4.13) to obtain an expression for $\dot{L}/M\dot{E}$, and to then expand Eqs. (3.31) and (3.32) in powers of e. The results are

$$\mu\dot{p} = -\frac{2p^{3/2}(p-3)^{3/2}}{p-6}\left\{1+O\left[\left(\frac{e}{p-6}\right)^2\right]\right\}\dot{E} \tag{4.14}$$

and

$$\mu\dot{e} = \frac{ep^{1/2}(p-3)^{1/2}}{2(p-2)(p-6)^2}\Big[p^3 - 12p^2 + 66p - 108 - 2\gamma(p-2)^2(p-6)\Big]\left\{1 + O\left[\left(\frac{e}{p-6}\right)^2\right]\right\}\dot{E}. \quad (4.15)$$

The detailed behavior of $\mu\dot{e}/e\dot{E}$ as a function of p depends on $\gamma(p)$, which must in general be evaluated numerically. However, since γ is well behaved in the limit $p \to 6$, the behavior of $\mu\dot{e}/e\dot{E}$ in that limit can be calculated unambiguously.

Taking the limit $p \to 6$ in Eqs. (4.14) and (4.15) we obtain

$$\mu\dot{p} = -\frac{108\sqrt{2}}{p-6}\left\{1 + O\left[p-6, \left(\frac{e}{p-6}\right)^2\right]\right\}\dot{E} \quad (4.16)$$

and

$$\mu\dot{e} = \frac{27\sqrt{2}}{(p-6)^2}e\left\{1 + O\left[p-6, \left(\frac{e}{p-6}\right)^2\right]\right\}\dot{E}. \quad (4.17)$$

Finally, substituting Eqs. (4.16) and (4.17) into (4.1) we arrive at

$$c(e,p) = -\frac{3}{2}\frac{1}{p-6}\left\{1 + O\left[p-6, \left(\frac{e}{p-6}\right)^2\right]\right\}. \quad (4.18)$$

The results presented here are consistent with our previous conclusion that radiation reaction acts on orbits which are close to the separatrix so as to decrease p and increase e. We also remark that for fixed μ/M, the divergence of $\mu\dot{p}$ and $\mu\dot{e}$ in the limit $p \to 6$ signals the breakdown of the adiabatic approximation. We will return to this point in Sec. IV D.

It should be emphasized that in both this and the preceding subsections, calculations were based on this property of circular orbits that $\dot{E} = \Omega_\phi \dot{L}$. This property is very general, and does not depend on the fact that the radiation field is gravitational [39]. That $\dot{E} = \Omega_\phi \dot{L}$ follows from two key elements. The first is that for circular orbits, the radiation field possesses a frequency spectrum of the form $\omega = m\Omega_\phi$. This follows from the circularity of the orbit only, and holds for any type of radiation field. The second key element is that irrespective of its type, the radiation field transports energy and angular momentum in such a way that for each frequency component, $\dot{E}_\omega \propto \omega$ and $\dot{L}_\omega \propto m$, where *the constant of proportionality is the same in both expressions* [39]. The equality $\dot{E} = \Omega_\phi \dot{L}$ is therefore valid for arbitrary radiation fields, and so are the results presented in this and the preceding subsections.

D. The adiabatic approximation

We now use the analytical estimates of the previous subsections to formulate constraints on μ/M which ensure the validity of the adiabatic approximation. These constraints are most severe in the vicinity of the separatrix. Due to the singularity of the transformation $\{\dot{E}, \dot{L}\} \to \{\dot{p}, \dot{e}\}$ at $p = 6+2e$, see Sec. III E, radiation reaction occurs increasingly rapidly as the orbit approaches the separatrix. Since $\dot{p}$ and $\dot{e}$ scale with μ/M, the validity of the adiabatic approximation can be maintained at the price of decreasing μ/M sufficiently rapidly. For a fixed mass ratio, the adiabatic approximation must eventually break down.

The adiabatic approximation is formulated by requiring that a relevant orbital parameter q changes very little over time scales comparable to the orbital period P. More precisely, we demand that

$$\Delta q \ll q, \quad (4.19)$$

where $\Delta q = |\dot{q}|P$ is the change in q after one radial orbit. By choosing q appropriately, and then estimating $\dot{q}$ and P, Eq. (4.19) can be transformed into a condition on μ/M.

1. The case $p \gg 6$

Expressions for $\dot{p}$ and $\dot{e}$ which are valid for large p are given by Eqs. (4.4) and (4.5). Using these results together with $P = 2\pi p^{3/2}(1-e^2)^{-3/2}M$, which is valid up to fractional corrections of order p^{-1}, Eq. (4.19) gives

$$\mu/M \ll p^{5/2}. \quad (4.20)$$

We note that Eq. (4.20) follows whether we choose $q \equiv p$ or $q \equiv e$. Equation (4.20) is superseded by the condition $\mu/M \ll 1$ which ensures that the gravitational perturbations obey linear wave equations. Thus, the adiabatic approximation is automatically satisfied in the weak-field limit.

We have already noted that the results presented in Sec. IV A are valid also for binary systems with arbitrary mass ratios, provided that μ is then interpreted as the reduced mass of the system, and M as the total mass. Since $\mu/M \leq 1/4$, with the equality holding when the masses are equal, we see that the radiation reaction is necessarily adiabatic when p is large, irrespective of the mass ratio.

2. The case $p - 6 - 2e \ll 4e$

The most relevant orbital parameter in this case is $q \equiv \varepsilon \equiv p - 6 - 2e$, and $\dot{\varepsilon}$ can be calculated using Eqs. (4.10) and (4.11). The orbital period can be expressed as $P = \Delta\phi/\Omega_\phi$ using Eqs. (2.18) and (2.19). Substitution of Eq. (2.32) then yields

$$\Delta\varepsilon \simeq 32\pi\frac{M}{\mu}\frac{(3-e)^{1/2}(6+2e)^2}{e(1+e)^{1/2}}\frac{\Delta\phi}{2\pi}\frac{\beta-\alpha}{\varepsilon}\dot{E}. \quad (4.21)$$

We now need to estimate $\beta - \alpha$, as well as $\dot{E}$. For the former, we recall Eq. (2.31) which shows that β is of the same order as $2\pi/\Delta\phi$, and the analysis of Sec. IV B which suggests that α is also of that order. We therefore write $\beta - \alpha \approx 2\pi/\Delta\phi$, where $\approx$ means "equal up to a

numerical factor of order unity." For $\dot{E}$ we use an estimate based on the quadrupole formula [5]; this estimate should be valid up to a numerical factor of order unity. Thus, $\dot{E} \approx (32/5)(\mu/M)^2(1+e)^5(6+2e)^{-5}$, which holds for a (fictitious) circular orbit of radius r_1. Gathering the results, and ignoring numerical factors, we arrive at

$$\mu/M \ll \varepsilon^2. \tag{4.22}$$

This condition on μ/M is indeed quite severe.

3. The case $p-6 \ll 1$; $e \ll p-6$

This case can be considered by identifying q with $p-6$, whose rate of change was evaluated in Sec. IV C. The orbital period is given by Eq. (2.36). We find,

$$\Delta(p-6) \simeq 7776\sqrt{2}\pi(p-6)^{-3/2}(M/\mu)\dot{E}. \tag{4.23}$$

Using the quadrupole formula to obtain the crude estimate $\dot{E} \approx (32/5)(\mu/M)^2 p^{-5}$, and ignoring numerical factors, we arrive at

$$\mu/M \ll (p-6)^{5/2}. \tag{4.24}$$

We remark, comparing Eqs. (4.22) and (4.24), that the rate at which μ/M must tend to zero as the point $(6,0)$ is approached varies with the direction of approach. This is an additional consequence of the fact that this point is a singular point of the p-e plane.

V. NUMERICAL RESULTS

In the first part of this section (Sec. V A–D) we will describe the numerical methods which were used to obtain the results presented in Figs. 1–3. We have written our code with the help of FORTRAN subroutines given in Ref. [40]. All computations were carried out with double precision.

In the final part of this section (Sec. V E) we will estimate the overall accuracy of our results, and compare them to those of Tanaka *et al.* [2].

A. The numerical task

The main function of our code is to compute, for a given point in the p-e plane, the numbers $Z^k_{\ell m}$ for each relevant ℓ, m, and k. This involves the numerical integration of Eq. (3.30), after the change of variables $r = r(\chi)$ has been made [see Eqs. (2.13) and (2.14)], and the evaluation of Eq. (3.29). The $Z^k_{\ell m}$ are then used to calculate $(M/\mu)^2\dot{E}$ and $(M/\mu)^2\dot{L}/M$ via Eqs. (3.12)–(3.14). Finally, these quantities are substituted into Eqs. (3.31) and (3.32), to obtain $M^2\dot{p}/\mu$ and $M^2\dot{e}/\mu$.

The computation of each $Z^k_{\ell m}$ involves many steps. These include the following.

(i) The evaluation of Ω_r and Ω_ϕ, which determine the perturbation frequency ω_{mk}. For this calculation we use Eqs. (2.15), (2.16), (2.18), (2.19), and (3.19).

(ii) The integration of the homogeneous Teukolsky equation [Eq. (3.3) with vanishing source], to obtain $R^H_{\omega_{mk}\ell}(\chi)$ for $0 \le \chi \le \pi$. From this we calculate ${}_sR^H_{\omega_{mk}\ell}(\chi)$, with the help of Eqs. (3.26)–(3.28). The integration of the homogeneous Teukolsky equation also gives $Q^{\rm in}_{\omega_{mk}\ell}$, the "amplitude" of the ingoing part of $R^H_{\omega_{mk}\ell}(r \to \infty)$, which is substituted into Eq. (3.29). Step (ii) is the one which requires the most care; it will be the subject of Sec. V C.

(iii) The computation of ${}_sG_\pm(\chi)$, $t(\chi)$, and $\phi(\chi)$, for $0 \le \chi \le \pi$. Equations (2.15), (2.16), and (3.21) are used for this calculation.

(iv) The evaluation of ${}_sp_\ell$, using Eq. (3.25), as well as ${}_sY_{\ell m}(\frac{\pi}{2},0)$, using Eq. (2.15) of Ref. [32].

The computation of $\dot{E}$ and $\dot{L}$ formally involves summing over an infinite number of terms. In Eq. (3.12), the sum over ℓ is only restricted by $\ell \ge 2$, and the sum over k is unrestricted. In Sec. V D we will examine the question of how to truncate these sums so as to achieve a desired degree of accuracy.

B. Integration of functions

Part of the numerical task involves the integration of several functions of χ, as is expressed in Eqs. (2.15), (2.16), and (3.30). Because these functions are all smooth, the integrations can be performed using Romberg's method, as implemented by the subroutine QROMB of Ref. [40].

The tolerance of the integrator, ϵ_R, can be set to very small values without difficulty. Thus, the numerical error introduced by the Romberg integrator can be chosen to be negligible compared to the truncation error (Sec. V D), which determines the overall accuracy of the final results. Typically we have chosen $\epsilon_R = 10^{-6}$.

When integrating Eq. (2.16) we have chosen *not* to take advantage of the fact that $\phi(\chi)$ can be written as an elliptic integral.

C. Integration of the homogeneous Teukolsky equation

A particularly important part of the numerical task is the integration of the homogeneous Teukolsky equation, Eq. (3.3) with vanishing source. We are interested in the particular solution $R^H_{\omega\ell}(r)$ which describes purely ingoing waves,

$$R^H_{\omega\ell}(r \to 2M) \sim (\omega r)^4 f^2 e^{-i\omega r^*}, \tag{5.1}$$

at the black-hole horizon. Here, $f = 1 - 2M/r$ and $r^* = r + 2M\ln(r/2M-1)$. At large distances,

$$R^H_{\omega\ell}(r \to \infty) \sim Q^{\rm in}_{\omega\ell}(\omega r)^{-1}e^{-i\omega r^*} + O\left(r^3 e^{i\omega r^*}\right), \tag{5.2}$$

where $Q^{\rm in}_{\omega\ell}$ is a constant. The function $R^H_{\omega\ell}(r)$ and its derivatives must be evaluated in the range $r_1 \le r \le r_2$. We must also estimate the "amplitude" $Q^{\rm in}_{\omega\ell}$. This is difficult, because the ingoing part of $R^H_{\omega\ell}(r)$ decays as

r^{-1} at large radii, while its outgoing part grows as r^3.

To avoid such complications [41], it is preferable to integrate, instead of the homogeneous Teukolsky equation, the related Regge-Wheeler equation [42]:

$$\left[f^2\frac{d^2}{dr^2}+\frac{2M}{r^2}f\frac{d}{dr}+\omega^2-W(r)\right]X_{\omega\ell}(r)=0, \quad (5.3)$$

where $W(r)=f[\ell(\ell+1)/r^2-6M/r^3]$. For this equation also we choose a particular solution $X^H_{\omega\ell}(r)$ which is purely ingoing at the black-hole horizon:

$$X^H_{\omega\ell}(r\to 2M)\sim\left[1+a_{\omega\ell}f+b_{\omega\ell}f^2+\cdots\right]e^{-i\omega r^*}, \quad (5.4)$$

where

$$a_{\omega\ell}=\frac{\ell(\ell+1)-3}{1-4iM\omega},$$
$$b_{\omega\ell}=\frac{(\ell-1)\ell(\ell+1)(\ell+2)-12iM\omega}{4(1-2iM\omega)(1-4iM\omega)}. \quad (5.5)$$

At large distances,

$$X^H_{\omega\ell}(r\to\infty)\sim A^{\rm in}_{\omega\ell}P_{\omega\ell}(\omega r)e^{-i\omega r^*}+A^{\rm out}_{\omega\ell}\bar{P}_{\omega\ell}(\omega r)e^{i\omega r^*}, \quad (5.6)$$

where $A^{\rm in}_{\omega\ell}$ and $A^{\rm out}_{\omega\ell}$ are constants, and $P_{\omega\ell}(\omega r)=1+\tilde{a}_{\omega\ell}(\omega r)^{-1}+\tilde{b}_{\omega\ell}(\omega r)^{-2}+\cdots$. Here

$$\tilde{a}_{\omega\ell}=-\frac{i}{2}\ell(\ell+1),$$
$$\tilde{b}_{\omega\ell}=-\tfrac{1}{8}\left[(\ell-1)\ell(\ell+1)(\ell+2)-12iM\omega\right], \quad (5.7)$$

and an overbar denotes complex conjugation.

From $X^H_{\omega\ell}(r)$ and its derivatives one recovers $R^H_{\omega\ell}(r)$ and its derivatives by applying the Chandrasekhar transformation [43],

$$R^H_{\omega\ell}(r)=4(b_{\omega\ell})^{-1}(M\omega)^3\omega r^2 f\mathcal{L}f^{-1}\mathcal{L}rX^H_{\omega\ell}(r), \quad (5.8)$$

where $\mathcal{L}=fd/dr+i\omega$. Because $X^H_{\omega\ell}(r)$ satisfies a second-order differential equation, the differentiations need not be performed numerically. The Chandrasekhar transformation also implies

$$Q^{\rm in}_{\omega\ell}=-4(1-2iM\omega)(1-4iM\omega)(M\omega)^3A^{\rm in}_{\omega\ell}. \quad (5.9)$$

From Eq. (5.8) one can indeed verify that $R^H_{\omega\ell}(r)$ satisfies the homogeneous Teukolsky equation, with boundary conditions (5.1) and (5.2), if $X^H_{\omega\ell}(r)$ is a solution to the Regge-Wheeler equation, with boundary conditions (5.4) and (5.6).

The numerical integration of Eq. (5.3) proceeds outward from $r=2M(1+\epsilon_I)$, where ϵ_I is a small number; typically $\epsilon_I=10^{-8}$. The integration is performed using the Bulirsh-Stoer method, as implemented by the subroutines ODEINT and BSSTEP of Ref. [40]. We have typically set the tolerance of the integrator to $\epsilon_{BS}=10^{-6}$.

The complex-valued amplitude $A^{\rm in}_{\omega\ell}$ is evaluated by integrating the Regge-Wheeler equation up to large values of r (large compared with the scale ω^{-1}), and by then comparing the numerical results with Eq. (5.6). More precisely, the integrator pauses at some r, estimates the value of $A^{\rm in}_{\omega m}$, and then proceeds to a larger value of r where another estimation is made. When $A^{\rm in}_{\omega m}$ changes by a fractional amount less than the imposed limit ϵ_A, the integrator stops and returns that value for $A^{\rm in}_{\omega m}$. In practice, the convergence of this process is quite rapid, thanks to the insertion of $P_{\omega\ell}(\omega r)$ in Eq. (5.6). However, we have found that in general, the required accuracy on $A^{\rm in}_{\omega m}$ must be set lower than the accuracy of the integrator. Otherwise, the estimator has difficulty converging at all; this convergence problem is more severe for larger frequencies. Typically, we have chosen $\epsilon_A=10\epsilon_{BS}$, which appears to work well for all values of p and e.

D. Truncation of infinite sums

As pointed out previously, the numerical calculation of $\dot{E}$ and $\dot{L}$ must involve the truncation of infinite sums over ℓ and k. This truncation obviously limits the accuracy of the numerical results. It is the purpose of this subsection to devise ways to truncate the sums so that the error introduced does not exceed a specified size.

It is easy to formulate a simple prescription for truncating the sums over ℓ. It was shown in Ref. [32] that for *circular* orbits, a given multipole ℓ contributes a fractional amount of order $p^{-(\ell-2)}$ to $\dot{E}$ and $\dot{L}$. We assume (and we have verified numerically) that this result remains valid, at least within an order of magnitude, when the orbit is eccentric. We then obtain that in order to achieve a fractional accuracy of order ϵ_ℓ, we must include in the sums over ℓ all terms with $\ell\le\ell_{\rm max}$, where

$$p^{-(\ell_{\rm max}-2)}\lesssim\epsilon_\ell. \quad (5.10)$$

We have found that Eq. (5.10) works indeed quite well in the region of the p-e plane which was of most interest to us. In principle, ϵ_ℓ could be chosen to be of the same order of magnitude as the previously introduced ϵ's. However, it is more appropriate to set it only slightly smaller than ϵ_k, which we define below, and which shall be the largest of the ϵ's.

It is more difficult to obtain a prescription for truncating the sums over k. First, it is necessary to know something about the distribution of $\dot{E}_{\ell mk}$ as a function of k, for fixed ℓ and m and for given values of p and e. The $\dot{L}_{\ell mk}$'s follow a similar distribution.

For very small eccentricities, the distribution of $\dot{E}_{\ell mk}$ is strongly peaked at $k=0$, and decays rapidly away from $k=0$. It can indeed be shown, using the equations of Sec. III, that for $e\ll 1$, $\dot{E}_{\ell mk}/\dot{E}_{\ell m0}=O(e^{2|k|})$; this analysis was carried out in Ref. [1].

For larger, but still small eccentricities (Fig. 5), the center of the distribution is pushed away from $k=0$ by an amount of order unity which depends on the values of p, e, ℓ, and m. However, it is still true that only a small number of k's make a significant contribution to $\sum_k\dot{E}_{\ell mk}$.

For large eccentricities (Fig. 6), a large number of har-

monics is required, and the center of the distribution is displaced from $k = 0$ by a large amount depending on the values of p, e, ℓ, and m. In all cases we have found that the negative values of k contribute very little to the total result.

Because the distributions of $\dot{E}_{\ell mk}$ and $\dot{L}_{\ell mk}$ as functions of k are so complex, it is not possible to truncate the sums over k at some universal values $k_{\min}$ and $k_{\max}$. Instead, for given p and e, and for fixed ℓ and m, we let the code compute $\dot{E}_{\ell mk}$ and $\dot{L}_{\ell mk}$ from $k = 0$ outward, comparing the value of the current $\dot{E}_{\ell mk}$ to the maximum value encountered thus far (for that ℓ and m). The calculation stops when for several successive k's, $\dot{E}_{\ell mk}$ drops below a fixed number ϵ_k times the maximum value. The calculation is then repeated for the negative k's, using the same maximum value. Finally, the sums over k are carried out, and the final answers for $\sum_k \dot{E}_{\ell mk}$ and $\sum_k \dot{L}_{\ell mk}$ are considered to have a fractional accuracy of order ϵ_k.

E. Overall accuracy

The overall accuracy of our results is determined, at least in part, by choosing the value of ϵ_k. A smaller value implies that more harmonics of the radial frequency will be included in the sums, which in turn implies a longer running time. For fixed ϵ_k, on the other hand, the running time increases rapidly with increasing eccentricity. Practically, therefore, it is not usually possible to set ϵ_k to very small values. We have typically chosen $\epsilon_k = 10^{-2}$. Fortunately, this relatively low accuracy is quite sufficient for our purposes.

Let ϵ denote the overall fractional accuracy of our results. The discussion of the preceding subsections implies the following hierarchy between all the ϵ's:

$$\epsilon \approx \epsilon_k \gtrsim \epsilon_\ell \gg \epsilon_A \gg \epsilon_{BS} = \epsilon_R \gg \epsilon_I. \tag{5.11}$$

To verify that ϵ_k is indeed a fair estimation of the overall accuracy, we have carried out runs with decreasing values of ϵ_k, and checked that the final answers differed by the expected amounts.

It is also useful, to assess our accuracy, to compare our results to the generally more accurate ones of Tanaka *et al.* [2]. Such a comparison was performed for several points in the p-e plane, and representative results are shown in Table I.

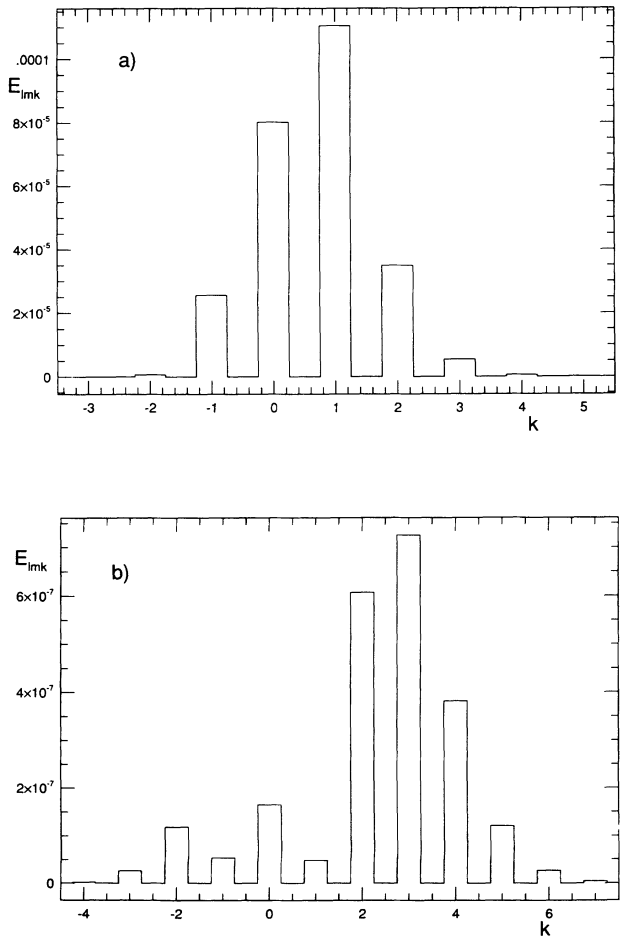

FIG. 5. The contributions $(M/\mu)^2\dot{E}_{\ell mk}$ to the total rate $(M/\mu)^2\dot{E}$, plotted as a function of the integer k, for fixed ℓ and m, and for $p = 7.50478$, $e = 0.188917$. See Eq. (3.12) and Table I. In part (a), $\ell = m = 2$. In part (b), $\ell = m = 5$.

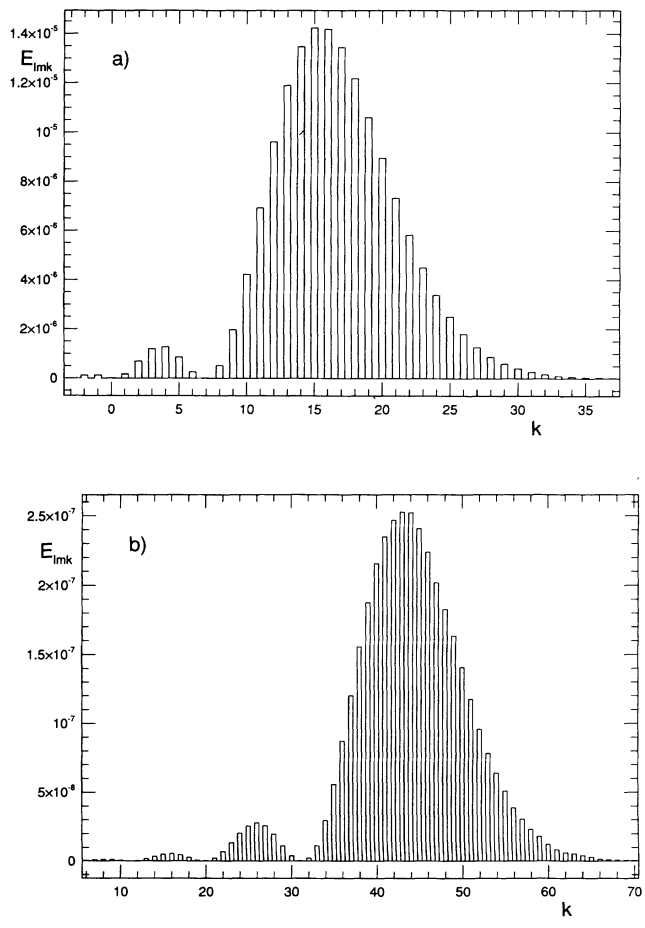

FIG. 6. The contributions $(M/\mu)^2\dot{E}_{\ell mk}$ to the total rate $(M/\mu)^2\dot{E}$, plotted as a function of the integer k, for fixed ℓ and m, and for $p = 8.75455$, $e = 0.764124$. See Eq. (3.12) and Table I. In part (a), $\ell = m = 2$. In part (b), $\ell = m = 5$.

TABLE I. Comparison with the results of Tanaka *et al.* for two representative points in the p-e plane. Shown are the values of p, e, $\tilde{E}$, $\tilde{L}$, r_1, r_2, Ω_r, Ω_ϕ, and $\Delta\phi$; the overall accuracy of our results (Tanaka *et al.* claim a fractional accuracy better than 10^{-4}); the values of $\dot{E}$ and $\dot{L}$ as calculated in this paper and by Tanaka *et al.*; the relative difference between the results; and the values of $\dot{p}$ and $\dot{e}$ as calculated in this paper.

Quantity	Point No. 1	Point No. 2
p	7.50478	8.75455
e	0.188917	0.764124
$\tilde{E}$	0.948279	0.977903
$\tilde{L}/M$	3.55000	3.85000
r_1/M	6.31228	4.96255
r_2/M	9.25279	37.1151
$M\Omega_r$	0.0210558	0.00804892
$M\Omega_\phi$	0.0475982	0.0153556
$\Delta\phi$	14.2036	11.9869
ϵ	10^{-4}	10^{-2}
$M^2\dot{E}/\mu^2$ (this paper)	3.16804×10^{-4}	2.10080×10^{-4}
$M^2\dot{E}/\mu^2$ (Tanaka *et al.*)	3.16689×10^{-4}	2.11580×10^{-4}
$M\dot{L}/\mu^2$ (this paper)	5.96562×10^{-3}	2.75034×10^{-3}
$M\dot{L}/\mu^2$ (Tanaka *et al.*)	5.96391×10^{-3}	2.76838×10^{-3}
Relative difference	4×10^{-4}	7×10^{-3}
$M^2\dot{p}/\mu$	-7.475×10^{-2}	-2.283×10^{-2}
$M^2\dot{e}/\mu$	-1.967×10^{-3}	-2.126×10^{-3}

As a final remark concerning the accuracy of our results, we note that we have not, in this paper, calculated $\dot{E}^H$ and $\dot{L}^H$, the time-averaged rates at which the black hole absorbs energy and angular momentum. Consequently, our results are only valid up to a fractional accuracy not better than $\epsilon_H \equiv \dot{E}^H/\dot{E}^\infty \approx \dot{L}^H/\dot{L}^\infty$, where $\dot{E}^\infty$ and $\dot{L}^\infty$ denote the rates at infinity. It can be shown [1] that for *circular* orbits, $\dot{E}^H/\dot{E}^\infty = \dot{L}^H/\dot{L}^\infty = O(p^{-4})$. We may assume that this result stays valid, at least within an order of magnitude, for eccentric orbits, and conclude that $\epsilon_H \approx p^{-4} < 8 \times 10^{-4}$. Because we have generally worked with $\epsilon \approx 10^{-2} \gg \epsilon_H$, we can safely ignore the contributions $\dot{E}^H$ and $\dot{L}^H$ to $\dot{E}$ and $\dot{L}$. This was also done by Tanaka *et al.* [2].

ACKNOWLEDGMENTS

For many helpful discussions we thank Amos Ori, Kip Thorne, Bill Unruh, and the members of the Caltech Relativity Group. For detailed comments on the manuscript we thank Eanna Flanagan. We also are grateful to Scott Hughes for much advice relating to our numerical computations. Part of these computations were performed at the Cornell Center for Theory and Simulation in Science and Engineering, which is supported in part by the National Science Foundation, IBM Corporation, New York State, and the Cornell Research Institute. The work presented here was supported by the National Science Foundation Grants No. AST 9114925 and AST 919475, and the National Aeronautics and Space Administration Grant No. NAGW-2897. E.P. acknowledges support from the Natural Sciences and Engineering Research Council of Canada. He is also grateful to Roberto Balbinot for his kind hospitality at the University of Bologna, where part of the analytical calculations were carried out.

[1] T. Apostolatos, D. Kennefick, A. Ori, and Eric Poisson, Phys. Rev. D **47**, 5376 (1993).
[2] T. Tanaka, M. Shibata, M. Sasaki, H. Tagashi, and T. Nakamura, Prog. Theor. Phys. **90**, 65 (1993).
[3] T. Damour, in *300 Years of Gravitation*, edited by S.W. Hawking and W. Israel (Cambridge University Press, Cambridge, England, 1987).
[4] W.L. Burke, J. Math. Phys. **12**, 401 (1971).
[5] C.W. Misner, K.S. Thorne, and J.A. Wheeler, *Gravitation* (Freeman, New York, 1973), Chap. 36.
[6] M. Walker and C.M. Will, Astrophys. J. **242**, L129 (1980).
[7] L. Blanchet and T. Damour, Phys. Lett. **104A**, 82 (1984).
[8] L. Blanchet, Phys. Rev. D **47**, 4392 (1993).
[9] B.R. Iyer and C.M. Will, Phys. Rev. Lett. **70**, 113 (1993).
[10] Here, we employ the phrase "post-Newtonian theory" to designate what is currently the state of the art of the field: a combination of a multipolar post-Minkowskian expansion for the metric outside the source, and a post-Newtonian expansion for the metric inside the source. The different expansions are matched in a region of common validity. For a summary of these methods, see [3]; L. Blanchet and T. Damour, Phys. Rev. D **46**, 4304 (1992); and references therein.
[11] Terms responsible for the radiation reaction first appear at order $(v/c)^5$ in the post-Newtonian expansion of the equations of motion.
[12] These sources are the most promising for the detection of gravitational waves by Earth-based interferometric detectors. For an overview, see C. Cutler, T.A. Apostolatos, L. Bildsten, L.S. Finn, E.E. Flanagan, D. Kennefick, D.M. Markovic, A. Ori, E. Poisson, G.J. Sussman, and K.S. Thorne, Phys. Rev. Lett. **70**, 2984 (1993).
[13] See, for example, P. Anninos, D. Hobill, E. Seidel, L. Smarr, and W.-M. Suen, Phys. Rev. Lett. **71**, 2851 (1993); E. Seidel and W.-M. Suen, *ibid.* **69**, 1845 (1992); and references therein.
[14] K. Danzmann, A. Rüdiger, R. Schilling, W. Winkler, J. Hough, G.P. Newton, D. Robertson, N.A. Robertson, H. Ward, P. Bender, J. Faller, D. Hils, R. Stebbins, C.D. Edwards, W. Folkner, M. Vincent, A. Bernard, B. Bertotti, A. Brillet, C.N. Man, M. Cruise, P. Gray, M. Sandford, R.W.P. Drever, V. Kose, M. Kühne, B.F. Schutz, R. Weiss, and H. Welling, "LISA: Proposal for a Laser-Interferometric Gravitational Wave Detector in Space," Max-Planck-Institut für Quantenoptik Report 177, May 1993 (unpublished).
[15] M.J. Rees, Nature (London) **333**, 523 (1988).
[16] D. Hils and P. Bender, "Gradual Approach to Coalescence for Compact Stars Orbiting Massive Black Holes" (unpublished).

[17] C. Cutler and E. Poisson (unpublished).
[18] D.V. Gal'tsov, J. Phys. A **15**, 3737 (1982).
[19] S. Chandrasekhar, *The Mathematical Theory of Black Holes* (Oxford University Press, New York, 1983).
[20] S.A. Teukolsky, Astrophys. J. **185**, 635 (1973).
[21] P.C. Peters, Phys. Rev. **136**, B1224 (1964).
[22] C.W. Lincoln and C.M. Will, Phys. Rev. D **42**, 1123 (1990).
[23] As the analysis of Secs. IV B and C implies, the essential reason for which the eccentricity increases near the separatrix is that the radiation reaction changes $\tilde{E}$ and $\tilde{L}$ so that $d\tilde{E} < \Omega\, d\tilde{L}$. Here, $\Omega = (M/r_1{}^3)^{1/2}$ is the angular velocity of a particle moving on a (fictitious) circular orbit of radius r_1.
[24] B. Carter, Phys. Rev. **174**, 1559 (1968).
[25] See, however, M. Shibata, Prog. Theor. Phys. **90**, 595 (1993).
[26] B.S. DeWitt and R.W. Brehme, Ann. Phys. (N.Y.) **9**, 220 (1960).
[27] F. Rohrlich, *Classical Charged Particles* (Addison-Wesley, Reading, 1965).
[28] This point was made clear to us by Amos Ori (personal communication).
[29] Y. Hagihara, Jpn. J. Astron. Geophys. **8**, 67 (1931).
[30] C.G. Darwin, Proc. R. Soc. London **A249**, 180 (1959); **A263**, 39 (1961).
[31] I.S. Gradshteyn and I.M. Ryzhik, *Table of Integrals, Series, and Products* (Academic, Orlando, 1980), Sec. 8.1.
[32] E. Poisson, Phys. Rev. D **47**, 1497 (1993).
[33] J.N. Goldberg, A.J. MacFarlane, E.T. Newman, F. Rohrlich, and E.C.G. Sudarshan, J. Math. Phys. **8**, 2155 (1967).
[34] M. Sasaki and T. Nakamura, Phys. Lett. **87A**, 85 (1981).
[35] S.L. Detweiler, Astrophys. J. **225**, 687 (1978).
[36] D.V. Galt'sov, A.A. Matiukhin, and V.I. Petukhov, Phys. Lett. **77A**, 387 (1980).
[37] M. Sasaki, Prog. Theor. Phys. **92** (1994).
[38] In the language of Ref. [1], $\gamma \equiv \Gamma/\dot{E}^{(0)}$.
[39] B. Carter, in *General Relativity: An Einstein Centenary Survey*, edited by S.W. Hawking and W. Israel (Cambridge University Press, Cambridge, England, 1979). The great generality of the relation $\dot{E} = \Omega_\phi \dot{L}$ was first recognized by Ya. Zel'dovich. We thank Kip Thorne for pointing this out to us.
[40] W.H. Press, B.P. Flannery, S.A. Teukolsky, and W.T. Vetterling, *Numerical Recipes* (Cambridge University Press, Cambridge, England, 1986).
[41] The method presented here is adapted from C. Cutler, L.S. Finn, E. Poisson, and G.J. Sussman, Phys. Rev. D **47**, 1511 (1993).
[42] T. Regge and J.A. Wheeler, Phys. Rev. **108**, 1063 (1957).
[43] S. Chandrasekhar, Proc. R. Soc. London **A343**, 289 (1975).

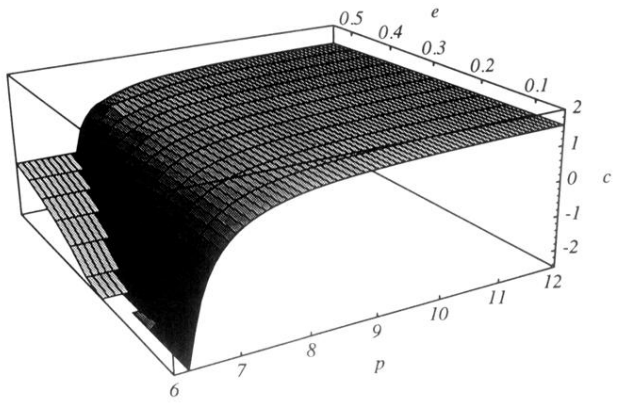

FIG. 2. A three-dimensional plot of the function $c(p,e) = d\ln e/d\ln p$, for the range $6 \leq p \leq 12$ and $0 \leq e \leq 0.55$. The function $c(p,e)$ is not defined for $p < 6+2e$. In this region we have plotted $\hat{c}(p,e) = -(1-e)/e$, which is equal to $c(p,e)$ at $p = 6+2e$; see Eq. (1.4). The intersection of the surface $c = c(p,e)$ with the plane $c = 0$ defines the critical curve, along which $de/dp = 0$; see Fig. 3. The value of $c(p,e)$ at the point $(7.5, 0.5)$ appears anomalous, but there is no reason to suspect the accuracy of our results at that point.